Diet modulates metabolic and hepatic responses to chronic pesticide mixture exposure in mice

C. Rives[1], N. Poirier-Jaouen[1], C.M.P Martin[1], M. Huillet[1], S. Ellero-Simatos[1], P. Perrier[1] A. Polizzi[1], F. Lasserre[1], V. Alquier Bacquié[1], C. Guyon[2], Y. Lippi[1], C. Naylies[1], E.L. Jamin[1,3], N.K Dieng[1,3], R. Vuillaume[1,3], C. Orlandi[1,3], J. Gomez[1], S. Costes[4], A. Arrar[4], A. Lucas[5], S. Fried[5], E. Boutet-Robinet[1], J. Guillermet-Guibert[2], E. Kesse-Guyot[6], H. Guillou[1], N. Loiseau[1], A. Fougerat[1,§] and L. Gamet-Payrastre[1,§].

1 Toxalim, Université de Toulouse, INRAE, ENVT, EI-Purpan, Toulouse, France.

2 Université de Toulouse, CNRS, Inserm, Centre de Recherches en Cancérologie de Toulouse (CRCT), Toulouse, France.

3 MetaboHUB-Metatoul, National Infrastructure of Metabolomics and Fluxomics, Metatoul-AXIOM, Toulouse, 31077, France.

4 IGF, Université Montpellier, CNRS, INSERM, Montpellier, France.

5 Institut des Maladies Métaboliques et Cardiovasculaires, INSERM, University Toulouse, UMR 1297-I2MC, We-Met facility, Toulouse, France.

6 Sorbonne Paris Nord University, Inserm, INRAE, Cnam, Nutritional Epidemiology Research Team (EREN), Epidemiology and Statistics Research Center-Paris Cité University (CRESS), Bobigny, France.

§ these authors share senior authorship

Corresponding author:

Laurence Gamet-Payrastre

Toxalim, Université de Toulouse, INRAE, ENVT, INP-Purpan, Toulouse, France.

laurence.payrastre@inrae.fr

Abstract

Chronic exposure to pesticide mixtures through diet is common, yet their combined metabolic effects and interactions with dietary factors remain unclear. We identified four pesticides prevalent in human exposure (imazalil, thiabendazole, boscalid, lambda-cyhalothrin) and assessed their combined impacts on hepatic metabolism and metabolic homeostasis using human liver cells and male mice fed standard chow or western diets. We found that the pesticide mixture induced metabolic perturbations in human hepatocytes. In addition, the pesticide mixture altered hepatic gene expression in chow-fed mice and exacerbated western diet-induced glucose intolerance, fasting hyperglycemia, and insulin resistance without affecting body weight or liver steatosis. These findings reveal that dietary context influences the metabolic consequences of pesticide mixtures, highlighting the need to consider nutritional status when evaluating environmental contaminant risks. Our results suggest that pesticide mixtures at reference doses may contribute to metabolic dysregulation, particularly under obesogenic dietary conditions.

Keywords

Chronic dietary exposure, Glucose homeostasis, Liver metabolism, Pesticide mixture, Metabolic effect

Highlights

- Four common pesticides in mixture disrupt metabolism in liver cells
- Dietary exposure to this pesticide mixture alters hepatic gene expression in mice
- The pesticide mixture exacerbates WD-induced disruptions in glucose homeostasis
- Pesticides and diet interact in producing the metabolic effects of a pesticide mixture

Introduction

Extensive use of pesticides in agriculture has contributed to the contamination of air, soil, water and food, exposing humans to these substances through multiple routes. There is growing evidence that exposure to several classes of pesticides may have adverse health effects in humans, particularly metabolic disorders (Expertise Collective Inserm 2021). Epidemiological studies have established a link between occupational exposure to pesticides and a higher incidence of obesity and type 2 diabetes (T2D) (Arab and Mostafalou 2023). Dietary pesticide exposure profiles have also been associated with T2D risk in the general population (Rebouillat et al. 2022). Conversely, higher consumption of organic foods—which typically contain lower levels of pesticide residues—has been associated with reduced risks of metabolic syndrome, obesity, and T2D (Baudry et al. 2018; Kesse-Guyot et al. 2017, 2020). However, although obesity and T2D are key risk factors for metabolic liver diseases such as metabolic dysfunction–associated steatotic liver disease (MASLD), and the liver is the main organ of pollutant metabolism, the link between pesticide exposure and MASLD development is less characterized (Rajak, S. et al. 2022).

Mechanistic studies suggest that several pesticides may interfere with pathways involved in metabolic regulation and liver function (Ahmad et al. 2024; Expertise Collective Inserm 2013), notably through interactions with hepatic nuclear receptors that regulate lipid and glucose metabolism, inflammation, and detoxification processes (Capitão et al. 2017; Fujino et al. 2019; Groswald et al. 2023; He et al. 2020; Knebel et al. 2018a, 2018b; Léger et al. 2023; Lichtenstein et al. 2020; Yang et al. 2023). Moreover, several *in vitro* and *in vivo* studies have reported the pro-oxidative properties of pesticides (Jabłońska-Trypuć 2017; Rives et al. 2020; Wang et al. 2022). Consistent with this, recent data suggest that exposure to certain organophosphate pesticides is associated with biomarkers of liver injury and function in humans (Li et al. 2022). Experimental studies further indicate that individual pesticides can disrupt overall metabolic homeostasis and promote hepatic steatosis (Arciello et al. 2013; Wahlang et al. 2019; Yang and Park 2018).

Dietary exposure to multiple pesticide residues is widespread, with consumers chronically exposed to complex mixtures at levels below regulatory limits (European Food Safety Authority (EFSA) et al. 2024; Baudry et al. 2021; Castorina et al. 2003). Yet, the simultaneous presence of multiple pesticides may yield additive or more than additive effects (Wang et al. 2023), which are not predicted by single-compound assessments (Cedergreen 2014; Christen et al. 2014; de Sousa et al. 2014; Roustan et al. 2014). These complex interactions have been mostly reported in *in vitro* models (Hernández et al. 2013; Schmidt et al. 2021; Tait et al. 2022; Lichtenstein et al. 2020; Wang et al. 2023). In recent years, preclinical studies have also supported the notion that mixed pesticides can alter metabolic homeostasis and liver function (Mesnage et al. 2021); Lukowicz et al. 2018).

85 Despite these advances, the metabolic consequences of chronic dietary exposure to realistic
86 pesticide mixtures, and their interaction with dietary factors remain unclear. In this study we
87 investigated the effects of chronic dietary exposure to a relevant pesticide cocktail at toxicological
88 references values on hepatic metabolism and energy homeostasis, and the potential interactions with
89 dietary factors.

90 Based on exposure profiles identified in the NutriNet Santé cohort (Baudry et al. 2021;
91 Rebouillat et al. 2021, 2022) and *in vitro* data, we selected four pesticides that induced, when
92 combined, metabolic perturbations in human liver cells. The pesticide mixture was then assessed for
93 its long-term effect in mice. The four pesticides were incorporated in a standard chow diet (CD) or in
94 a western diet (WD) at doses allowing mice to be exposed for 20 weeks to two reference doses: the
95 human acceptable daily intake (ADI; an estimate of the amount that can be ingested on a daily basis
96 over a lifetime without appreciable risk to human health) or a tenfold higher dose (10ADI or 1/10
97 NOAEL; one-tenth of the no-observed-adverse-effect level, the highest experimentally determined
98 dose at which no statistically or biologically significant effect has been described), for each of the four
99 individual pesticides. Our murine findings provide evidence that exposition to toxicological reference
100 values of each pesticide in mixture can induce molecular and phenotypic effects in a diet specific
101 manner.

102 **Materials and Methods**

103 1. Chemical and reagents

104 All pesticides used were of 98% purity (Sigma-Aldrich, France). Stock solutions at 50 mM were prepared
105 in >99% dimethyl sulfoxide (DMSO, Sigma-Aldrich, France) and stored at −20°C. The designation ITBL
106 5, 15 or 30 indicates that each pesticide (imazalil [IMZ], thiabendazole [TBZ], boscalid [BSC], lambda-
107 cyhalothrin [LCT]) in the mixture was at 5, 15 or 30 µM. LC–MS grade methanol (MeOH) and acetic acid
108 were purchased from Fisher Scientific (Illkirch, France). Ultrapure water was produced using a Milli-Q
109 system (Millipore, Saint-Quentin en Yvelines, France).

110

111 2. Cell culture and pesticide treatments

112 Immortalized human hepatocytes (IHH) were a generous gift from Professor Bart Staels (Institute
113 Pasteur, Lille, France; Samanez et al. 2012). Cells were seeded in 6- or 12-well plates precoated with 1
114 g/L porcine gelatin (Sigma-Aldrich) in William's medium(Gibco) (10% decomplemented fetal calf
115 serum, Dutscher), penicillin (100 units/mL, Sigma-Aldrich), and streptomycin (0.1 mg/mL, Sigma-
116 Aldrich), glutamine (4 mM, Sigma-Aldrich), dexamethasone (1 nM, Supelco), and bovine insulin (8.4
117 nM, Sigma-Aldrich) at 37°C with 95% humidity and 5% CO_2. Fifteen hours after seeding, cells were
118 cultured in Dulbecco's Modified Eagle Medium (DMEM) (pyruvate 230 µM, bovine serum albumin
119 [BSA] 1 g/L, penicillin 100 units/mL, and streptomycin 0.1 mg/mL [Sigma-Aldrich], glutamine 4 mM
120 [Sigma-Aldrich], dexamethasone 1 nM [Supelco], Gibco) without serum for 6 hours. Subsequently, cells
121 were cultured in DMEM supplemented with 4% fetal calf serum, human insulin (0.1 to 1 nM) (Sigma-
122 Aldrich), and glucose (Sigma-Aldrich) (1 mM to 4 mM) according to the experiments and treated with
123 a 1000-fold concentrated solution of the mixture of the four pesticides (ITBL), in dimethyl sulfoxide
124 (DMSO, Sigma-Aldrich). Controls were cells exposed to 0.1% DMSO.

125

126 3. Cell viability

127 IHH cells were seeded in 12-well plates (1×10^5 cells/well) and treated either for 24 hours, 72 hours or
128 10 days at 5, 15, 30 µM with each pesticide alone. For the 10-day treatment, the medium was changed
129 every 48 hours. At the end of the experiment, the cells were collected upon trypsin treatment (Sigma-
130 Aldrich), and were counted using the Luna IITM cell counter after staining with trypan blue (Sigma-
131 Aldrich).

132

133 4. Neutral lipid quantification in IHH cells and liver samples

134 IHH cells were seeded in 6-well plates (2.8×10^5 cells/well) and treated every 2 days for 10 days with
135 the pesticide mixture (ITBL) at 30 µM. The agonist of the liver X receptor (LXR), T-0901317 (T0, 30 µM,
136 Sigma-Aldrich), was added 24 hours before cell recovery and was used as a positive control for

137 intracellular neutral lipid quantification. After 10 days of treatment, cells were harvested (2 wells were
138 pooled) by scraping in EGTA (aqueous solution) 5 mM: methanol (1:2, v/v). For mouse liver samples,
139 the equivalent of 2 mg of tissue was homogenized in FastPrep tubes containing beads and aqueous
140 EGTA 5 mM:methanol (1:2, v/v), then processed using a Precellys, as described previously (Bligh and
141 Dyer, 1959).
142 Lipid extraction was performed by adding 2.5 mL of methanol (Sigma-Aldrich), 2 mL of Milli-Q water,
143 and 2.5 mL of dichloromethane (Fisher Chemical) (2.5:2.5:2, v/v/v) to cell and liver samples. For cells,
144 evaporation was performed twice before resuspending the extracts in 20 µL of ethyl acetate (Sigma-
145 Aldrich). For liver samples, a single evaporation was performed before resuspending the extracts in
146 160 µL of ethyl acetate. A standard mixture composed of 6 µg of stigmasterol (2 µg/10 µL), 6 µg of
147 cholesterol C17 (2 µg/10 µL), and 16 µg of triglycerides TG19 (4 µg/10 µL) was used. Lipids
148 (triglycerides, free cholesterol, and cholesterol esters) were quantified by gas chromatography coupled
149 with flame ionization detection (GC-FID) (Lipidomics Platform, I2MC, Toulouse), using a Thermo
150 Electron system focused with a Zebron-1 Phenomenex fused silica capillary column (5 m, 0.32 mm
151 internal diameter, 0.50 µm film thickness; Phenomenex, England), as previously described (Podechard
152 et al. 2018). The oven temperature was programmed to increase from 200°C to 350°C at a rate of
153 5°C/min, and the carrier gas was hydrogen (0.5 bar). The injector and detector were set at 315°C and
154 345°C, respectively.
155
156 5. Measurement of mitochondrial oxygen consumption rate
157 IHH cells were treated for 24 hours with the pesticide mixture (ITBL) at 30 µM in DMEM medium (XFe24
158 Cell Culture Microplates pre-coated with gelatin, 6.25×10^5 cells/well). Then, cells were incubated in
159 Seahorse XF DMEM Medium, pH 7.4 (Agilent) (Seahorse XF Glucose (1 mM final), Seahorse XF Pyruvate
160 (0.1 mM final), and Seahorse XF L-Glutamine (0.2 mM final). Real-time measurements of the oxygen
161 consumption rate (OCR) were performed by isolating a small volume (approximately 5 µL), also known
162 as a "transient microchamber", above the cell monolayer using the Seahorse XF Cell Mito Stress Test
163 (Agilent, Santa Clara, CA, US).
164 Through an integrated drug delivery system, three compounds were sequentially added to the wells
165 (30-minute intervals between each injection): oligomycin (2 µM, ATP synthase inhibitor), carbonyl
166 cyanide-4 (trifluoromethoxy) phenylhydrazone (FCCP, 2 µM, mitochondrial uncoupler),
167 rotenone/antimycin A (0.5 µM each, inhibitors of complex III of the respiratory chain), to determine
168 ATP production, maximal respiration, and proton leak, respectively. Data were analyzed using
169 Seahorse XFe Wave software (Agilent). The data were normalized to the cell density in each well
170 measured by an automated IncuCyte cellular imaging system (Sartorius).
171

172 6. Animals and diets

173 *In vivo* studies were conducted in accordance with EU directive 2010/63/EU for animal experiments
174 and approved by an independent ethics committee under authorization number 17430-
175 2018110611093660. All mice were housed at 21–23°C with a 12h/12h light/dark cycle and had access
176 to standard rodent chow diet (SAFE A04 U8220G10R from SAFE Augy, France) and tap water. Eight-
177 week-old male SOPF C57BL/6 mice (Janvier Labs) were acclimatized for one week and then randomly
178 assigned to different experimental groups. Mice were fed either a standard chow diet (CD; 70%
179 carbohydrate, 4% fat, and 14% protein, n = 36) or a Western diet (WD; 61% carbohydrate, 20% fat, and
180 14% protein, n = 36) *ad libitum*. After 5 weeks, both groups were further divided into 3 subgroups: (i)
181 a group fed a diet containing the mixture of 4 pesticides (ITBL) and exposed to the acceptable daily
182 intake (CD-ADI or WD-ADI) of each pesticide; (ii) a group fed a diet containing the mixture of 4
183 pesticides (ITBL) and exposed to 10ADI, corresponding to 10 times the ADI (CD-10ADI or WD-10ADI),
184 of each pesticide; and (iii) one group not exposed to pesticides (CD or WD). The exposure period lasted
185 for 20 weeks (n = 12 animals/group). Rodent diets were prepared in collaboration with the SAAJ unit
186 (Jouy-en Josas) as described previously (Lukowicz et al. 2018). The quantities of pesticides incorporated
187 into the rodent diet were confirmed by LC-MS analysis (Eurofins, France) (supplementary Table 1).
188 Body weight, food intake, and water consumption were monitored weekly throughout the experiment.
189

190 7. RNA extraction of IHH cells and liver samples

191 IHH cells (2×10^5 cells/well, 6 well-palte) and treated for 24 hours with the mixture (ITBL) at 30 µM.
192 The cell monolayers or the liver samples were lysed using TriReagent (MRC). After addition of
193 chloroform (Fisher Chemical), total RNAs were extracted in the aqueous phase and then precipitated
194 with 99.8% isopropanol (Sigma-Aldrich. After washing with 70% ethanol (Sigma-Aldrich), the RNA was
195 resuspended in RNase/DNase-free water (Ambion). The RNA concentration was measured using a
196 nanophotometer (Nanodrop 1000, Thermo Scientific) at an absorbance of 260 nm. The RNA was
197 diluted to a concentration of 135 ng/µl for microarray analysis (IHH cells) or RNA sequencing (liver
198 samples).
199

200 8. Gene expression analysis

201 a. Quantification of relative mRNA expression by RT-qPCR

202 To perform real-time quantitative PCR, 2 µg of RNA was reverse transcribed using a High-Capacity
203 cDNA Reverse Transcription Kit (Applied Biosystems, Foster City, CA, USA). Amplification reactions
204 were carried out in 96-well plates in a mixture consisting of SYBR Green (Low ROX SYBR MasterMix
205 dTTP blue, Takyon), a fluorescent DNA intercalating agent, primer pairs of interest at a final
206 concentration of 300 nM or 900 nM depending on primer efficiency, and cDNA diluted to a 1:20 ratio

207 in ultrapure DNase/RNase-free water. The primer sequences used are presented in supplementary
208 Table 2.
209 qPCR experiments were performed using an AriaMx real-time PCR system (Agilent). Fluorescence data
210 were analyzed using LinRegPCR software to calculate the PCR efficiency per point and provide a relative
211 initial mRNA concentration through linear regression of the exponential phase of the PCR curve. The
212 relative expression measurements of the genes of interest were normalized to the expression level of
213 the mRNA encoding the GAPDH protein (glyceraldehyde-3-phosphate dehydrogenase).

214 b. Gene expression profiling of IHH cells by microarray

215 Gene expression profiles were obtained for six different cell passages (p26 to p31) on the GeT-TRiX
216 platform (GenoToul, Genopole Toulouse Midi-Pyrénées) using Agilent SurePrint G3 Human GE v3 DNA
217 microarrays (8 × 60K, model 072363) following the manufacturer's instructions. Microarray data
218 acquisition was achieved from 200 ng of total RNA as described previously (Lukowicz et al. 2018).
219 Microarray data and experimental details are available in the Gene Expression Omnibus (GEO)
220 database at NCBI (GSE305353).
221 Microarray data were analyzed using R (https://www.R-project.org) and Bioconductor packages
222 (Huber et al. 2015) as described previously (Lukowicz et al. 2018). Enrichment analysis for biological
223 processes in the gene ontology (GO) was performed using Metascape (Zhou et al. 2019), and
224 transcription factor enrichment was assessed using TRRUST.

225 c. Gene expression profiling of liver samples by RNA sequencing

226 For each of 66 samples, RNA-seq libraries were constructed from 1000 ng of total RNA at the GeT-TRiX
227 facility (GénoToul, Génopole Toulouse Midi-Pyrénées) using an Illumina Stranded mRNA Prep kit
228 (Illumina, San Diego, CA, USA) following the manufacturer's instructions adapted to produce library
229 sizes compatible with paired-end 150-bp read-length sequencing. The libraries were then pooled to
230 equimolar concentrations and transferred to the GeT-PlaGe facility (GénoToul, Génopole Toulouse
231 Midi-Pyrénées) for sequencing into one lane on an Illumina NovaSeq 6000 using a 2 × 150-bp paired-
232 end sequencing mode with a NovaSeq 6000 S4 Reagent Kit v1.5.
233 Bioinformatics treatment was executed with Nextflow v23.10.0-edge (Di Tommaso et al. 2017) and
234 processed using nf-core/rnaseq v3.14.0 (https://doi.org/https://doi.org/10.5281/zenodo.1400710) of
235 the nf-core collection of workflows (Ewels et al., 2020). Reads were aligned to human genome
236 reference GRCm39 (build GCA_000001635.9, release: 2023-04). Sequencing data and experimental
237 details are available in NCBI's Gene Expression Omnibus (Edgar et al., 2002) and are accessible through
238 GEO Series accession number (to be provided).
239 Biostatistics analyses were performed under R v4.3.0 (R Core Team, 2023) as previously described
240 (Chousidis et al. 2025).

241 Clustering results are shown as a heatmap of expression signals, using the MATRIX application (Lippi
242 and Soubès 2023), based on differentially expressed genes ($p \leq 0.05$ and fold change >1). Gene
243 Ontology (GO) enrichment analysis of Biological Processes was performed using Metascape (Zhou et
244 al. 2019) with FDR <5%, using default settings.
245
246 9. Blood and tissue samples
247 Blood samples were collected from the submandibular vein into lithium heparin–coated tubes
248 (Sarstedt, Nümbrecht, Germany) throughout the experiment (weeks 12, 16 and at the time of
249 euthanasia). Plasma was isolated by centrifugation (1500 g, 15 min, 4°C) and stored at −80°C. Following
250 animal euthanasia by cervical dislocation, tissue samples were collected, weighed, dissected, and used
251 for histological analyses or frozen in liquid nitrogen and stored at −80°C until further use.
252
253 10. Oral glucose tolerance test (OGTT) and plasma insulin concentration
254 The OGTT was conducted after 23 weeks of diet. Mice were fasted for 6 hours before receiving a
255 glucose solution (2 g/kg body weight) by gavage. Blood glucose levels were measured from the tail
256 vein using an Accu-Check Performa glucometer (Roche Diabetes Care France, Mylan, France) 30
257 minutes before and 0, 15, 30, 60, 90, and 120 minutes after receiving the glucose solution. For
258 measurements of plasma insulin concentration (see plasma biochemical analyses), 20 µL of blood was
259 drawn from the tip of the tail vein 30 minutes before and 15 minutes after glucose gavage.
260
261 11. Plasma biochemical analyses
262 The plasma insulin concentration was measured using the We-Met platform (I2MC, Toulouse,
263 France) with an Insulin Mouse Serum Assay HTRF kit (Revvity). During weeks 5, 12, 16, and 23, fasting
264 blood glucose (6 hours of fasting) was measured from a drop of blood taken from the tail vein, using
265 an Accu-Check Performa glucometer (Roche Diabetes Care France, Mylan, France). Plasma samples
266 were analyzed to determine the levels of alanine aminotransferase (ALT), using a Cobas Mira Plus
267 biochemical analyzer (Roche Diagnostics, Indianapolis, IN, USA) (ANEXPLO facility, Toulouse, France).
268
269 12. Histology
270 Paraformaldehyde-fixed, paraffin-embedded liver tissue sections (3 µm) were stained with
271 hematoxylin and eosin (H&E) for histopathological analysis ($n = 12$ per group). The stained liver
272 sections were analyzed blindly for steatosis. The histological features were grouped with the steatosis
273 score evaluated according to Akpolat et al. (Akpolat et al. 2005).
274 Paraformaldehyde-fixed, paraffin-embedded pancreas tissue sections (4 µm–thick longitudinal
275 sections) were stained with H&E, scanned with a Pannoramic 250 Flash III microscope, and analyzed

276 in blinded fashion (n = 6 per group). The number of islets were quantified and the area of each islet
277 was measured with NDP.view software, version 2.9.29 (Hamamatsu).
278
279 13. Analysis of pesticides and their metabolites in urinary samples
280 Urinary samples were collected during 24 h the week before euthanasia and stored at −80°C. Analysis
281 of pesticides and their metabolites are described in supplementary Table 3.
282
283 14. Statistical analysis
284 Statistical analyses were performed using GraphPad Prism for Windows (version 10.2.; GraphPad
285 Software). Data are presented as mean ± SEM. *In vitro* data were normalized to the total mean of each
286 experiment before being pooled, with two exceptions: intracellular triglyceride measurements where
287 the data were normalized to the number of cells in each condition before pooling; and the heatmap of
288 genes linked to liver steatosis, hepatotoxicity, and nuclear receptor activation, where the data were
289 normalized to control gene expression. For all experiments in IHH cells, effects were assessed with
290 unpaired t-test, excepted for oxygen consumption rate (OCR) the effects were assessed with two-way
291 ANOVA followed by Tuckey's post-hoc test. For all animal experiments, differential effects were
292 assessed with one-way ANOVA followed by Tuckey's post-hoc test, excepted for body weight survey
293 and the oral glucose tolerance test (OGTT) a two-way ANOVA followed by Tuckey's post-hoc test was
294 performed. For histology experiments and urinary metabolites analysis differential effects were
295 assessed with Kruskal–Wallis followed by Dunn's multiple comparisons test.
296
297
298
299
300
301
302
303
304
305
306
307
308
309
310

311 **Results**

312 **1. Selection of candidate pesticides**

313 We established a list of candidate pesticides to be further evaluated for their effects on hepatic
314 metabolism. We first used recent results from a prospective cohort that characterized the dietary
315 exposure profiles to pesticides in a large sample of French adults with variable consumer habits. This
316 study identified six different exposure clusters in regard to estimated dietary exposure to 25 commonly
317 used pesticides (Rebouillat et al. 2021). In the most exposed cluster ("cluster 3"), we selected the 12
318 pesticides with highest estimated exposure (Rebouillat et al. 2021) (Figure 1). We next refined our
319 selection by examining which of those 12 pesticides have a mode of action on their target organisms
320 linked to oxidative stress and lipid metabolism (Leroux 2003; https://irac-online.org/mode-of-
321 action/classification-online/), two key events in the development and progression of metabolic liver
322 diseases (Friedman et al. 2018). This second selection led to a list of nine pesticides. Among them,
323 three pesticides that were banned according to the pesticide use regulations in the European Union
324 (EPHY – ANSES & the EU pesticide database) were excluded. The remaining six pesticides belong to
325 four different classes: a pyrethroid insecticide (lambda-cyhalothrin), a fungicide from the strobilurin
326 class (azoxystrobin), a fungicide from the carboxamide class (boscalid), and three azole fungicides
327 (imazalil, thiabendazole, and tebuconazole). Finally, among the three azole pesticides, we examined
328 those that recently showed positive association with T2D risk in the same French NutriNet-Santé
329 cohort (Rebouillat et al. 2022), as MASLD is frequently associated with diabetes (Stefan & Cusi, Lancet
330 Diabetes Endocrinol, 2022). This led to a final list of five pesticides, including four fungicides
331 (azoxystrobin [AZX], boscalid [BSC], imazalil [IMZ], thiabendazole [TBZ]) and one insecticide (lambda-
332 cyhalothrin [LCT]) (Figure 1).

333 *In vitro* exposure concentrations were derived from the ADI value of each pesticide. Estimated blood
334 concentrations were calculated assuming a 60kg individual with a 5L blood volume, resulting in
335 estimated concentrations in the micromolar range. Accordingly, the four compounds were tested at 5,
336 15 and 30 µM.

337 Our preliminary experiments on IHH cellular viability revealed that IMZ, TBZ, BSC, and LCT did not
338 drastically alter cell viability in response to acute (24 h), or subchronic (72 hours or 10 days) exposure
339 to increasing concentrations of individual pesticides (supplementary Figure 1A-C). AZX induced
340 cytotoxicity at concentrations as low as 5 µM after 72 hours of exposure (supplementary Figure 1B)
341 and was therefore excluded. Subsequent experiments were conducted using the four pesticides at 30
342 µM, the highest non-cytotoxic dose for both acute and chronic exposure in IHH cells.

343
344 **2. Effects of the mixture of 4 pesticides on hepatic metabolism *in vitro***

345 We next assessed the effects of the 4 selected pesticides in mixture on IHH lipid metabolism and
346 oxidative stress, two key events in the development and progression of obesity-associated hepatic
347 disease (Mardinoglu 2018). We performed several *in vitro* assays in IHH cells targeting molecular
348 initiating and key biological events of the adverse outcome pathway (AOP) for liver steatosis (AOP 34,
349 36, 57, 58, 517, 518 https://aopwiki.org) (supplementary Figure 2) (Mellor et al. 2016; Vinken et al.
350 2017).
351 We first evaluated the activation of the nuclear receptors PPARα, CAR, PXR, LXR and of the
352 transcription factor AhR (the main molecular initiating event triggering liver steatosis (supplementary
353 Figure 2)) by measuring the relative expression of their respective target genes *CYP4A11*, *CYP2B6*,
354 *CYP3A4*, *SREBP1c*, and *CYP1A1* in IHH cells exposed for 24 h to 30 µM of each pesticide in the mixture.
355 IHH cells exposed to the mixture of the 4 pesticides presented with a significantly higher expression of
356 CYP2B6, CYP3A4, SREBP1 and CYP1A1 compared to untreated cells suggesting activation of CAR, PXR
357 LXR and AhR respectively (Figure 2A).
358 Nuclear receptor activation induces changes in gene and protein expression which are considered key
359 biological events in the steatosis AOP. Thus, we used an untargeted microarray approach to examine
360 the whole pattern of IHH gene expression upon pesticide exposure and investigated the differences in
361 gene expression between untreated IHH cells and those exposed to the mixture of the four compounds
362 (Figure 2 B-E). Principal Component Analysis showed a clear discrimination between untreated and
363 pesticide-treated IHH cells (Figure 2B). In addition, the number of differentially up- and down-
364 regulated genes (DEGs) was increased in cells exposed to the pesticide mixture compared to control
365 non-exposed cells (Figure 2C). Hierarchical clustering of DEGs ($p<0.05$ and fold change >1.5, 4205
366 genes) highlighted two clusters with gene expression levels that differed between unexposed IHH cells
367 and those exposed to the pesticide mixture (Figure 2D). Genes from cluster 1 were downregulated in
368 cells exposed to the pesticide mixture and were linked to cell cycle processes and enriched in E2F1/4,
369 MYC, and TP53 target genes. Genes from cluster 2 were upregulated in cells exposed to the pesticide
370 mixture and are mainly targets of SP1, STAT3, TP53, and ATF4 transcription factors. The top related
371 biological functions were “response to nutrient levels”, “nuclear receptor meta pathway”, “negative
372 regulation of intracellular signal transduction”, and “response to endoplasmic reticulum stress” (Figure
373 2E). We then focused our analysis on relevant genes involved in liver steatosis, nuclear receptor
374 activation, and hepatotoxicity (Lichtenstein et al. 2020). As shown in supplementary Figure 3, IHH
375 exposure to the pesticide mixture led to significant upregulation of a large number of these genes,
376 relative to gene expression in untreated cells. The most strongly induced genes are involved in
377 xenobiotic metabolism (*SULT1C2*, *CYP3A5*, *UGT2B7*, *CYP2B6*, *POR*) and in lipid metabolism (*PNPLA3*,

378 *SCD1*, *SREBF1*, *MSMO1*, *PPARα*, *HADHB*), supporting the potential pro-steatotic impact of the pesticide
379 mixture.
380 We next measured intracellular triglyceride levels in IHH cells treated for 10 days with the pesticide
381 mixture using GC-FID as lipid accumulation is a key event in the AOP for liver steatosis and a hallmark
382 of the disease. Exposure of IHH cells to the pesticide mixture at 30 µM resulted in a higher content of
383 triglycerides compared with that of untreated cells (Figure 2F).
384 At the organelle level, mitochondrial disruption has been proposed to be a late key event in the
385 steatosis AOP. Thus, we next evaluated the effect of combined pesticides on IHH cell mitochondrial
386 respiratory functions using Seahorse XF stress test technology. Exposure of IHH cells to the pesticide
387 mixture led to an increased basal and maximal mitochondrial respiration (Figure 2G) and a significant
388 rise in ATP production (Figure 2H).
389 Altogether, combining data from previously published epidemiological studies and a panel of *in vitro*
390 assays, we identified four commonly used pesticides that, when combined, induced metabolic
391 perturbations in liver cells.
392
393 **3. Chronic dietary exposure to the mixture of 4 pesticides in mice**

394 We next investigated the *in vivo* metabolic and hepatic effects of the pesticide mixture and the
395 interactions with dietary factors. Adult male mice were first fed either a control diet (CD) or a western
396 diet (WD) for 5 weeks and then exposed to the pesticide mixture through these diets for an additional
397 20 weeks (Figure 3A). Pesticides were incorporated in the CD and WD at doses exposing mice to the
398 ADI (CD- or WD-ADI) or 10 times ADI (CD- or WD-10ADI) of each of the four pesticides in the mixture
399 (Figure 3A). Pesticide levels quantified in the feed pellets confirmed that the concentration of the four
400 pesticides in each diet was close to the expected quantities (supplementary Table 1).

401 Body weight did not show any significant differences between exposed (ADI and 10ADI) and non-
402 exposed mice in both the CD- and the WD-fed groups (Figure 3B, C). Perigonadal (WATpg) and
403 subcutaneous (WATsc) white adipose tissue weights were also not significantly changed by pesticide
404 mixture exposure in mice fed a CD or WD, except for a small increase in the relative WATsc weight in
405 the CD-10ADI compared with that in the CD mice (Figure 3D-G). Food and water intake also did not
406 differ between exposed and unexposed mice in both the CD- and the WD-fed mice (supplementary
407 Figure 4A, B).

408 We next evaluated the impact of pesticide mixture exposure on liver homeostasis during CD and WD
409 feeding. Animal exposure to the pesticide mixture did not impact liver weight nor induce hepatic
410 damage, whatever the dose and the type of diet (CD or WD) (Figure 4A-D). Histological analysis of H&E-

411 stained liver slices and hepatic triglyceride quantification confirmed the absence of pesticide impact
412 on hepatic steatosis in WD-fed mice (Figure 4E, F). By contrast, a slight but significant increase in the
413 steatosis score and a trend toward higher hepatic triglyceride levels were observed in CD-ADI–fed mice
414 compared with unexposed mice (Figure 4E, F).

415 To further explore the potential impact of pesticide exposure on the liver, we analyzed the hepatic
416 transcriptome in each animal group using RNA sequencing. PCA of gene expression profiles showed a
417 slight separation between exposed and non-exposed mice fed a CD along the first principal
418 component, accounting for 19.4% of the variance (Figure 4G). By contrast, PCA did not allow
419 discrimination between exposed and non-exposed WD-fed mice, whatever the dose of pesticide
420 mixture (Figure 4H). The number of differentially up- and down-regulated genes in CD-fed mice
421 exposed to the ADI of each pesticide in the mixture (607 up- and 611 down-regulated genes) and to
422 10ADI of each pesticide in mixture (904 up- and 994 down-regulated genes) was higher than it was in
423 unexposed animals (Figure 4I). By contrast, exposure to the pesticide mixture in WD-fed mice did not
424 affect the number of DEGs compared with that in the unexposed animals. We performed hierarchical
425 clustering of DEGs ($p<0.05$ and fold change >1; 2311 genes) in the CD, CD-ADI, and CD-10ADI groups
426 (Figure 4J). Two clusters of genes were identified. Genes from clusters 1 and 2 were respectively up-
427 and down-regulated in exposed CD-fed (CD-ADI and CD-10ADI) compared with their expression in
428 unexposed CD-fed mice (Figure 4J). Upregulated genes are linked to fatty acid metabolism, amino acid
429 metabolism, and cellular respiration, and are mainly enriched in PPARα targets. Downregulated genes
430 from cluster 2 are mainly involved in RNA and protein processing (Figure 4K).

431 Altogether, liver analysis showed that exposure to the pesticide mixture did not exacerbate WD-
432 induced alterations in hepatic phenotype and gene expression. However, exposure to the pesticide
433 mixture in CD-fed mice was associated with significant changes in hepatic gene expression.

434 To further investigate the differential hepatic impact of pesticide exposure according to the type of
435 diet, we compared pesticide metabolism in CD- and WD-fed mice. Analyses of urine samples by UHPLC-
436 HRMS allowed the detection of several pesticides and their metabolites. As shown in Figure 5A-D and
437 supplementary Table 3, TBZ and BSC and 3 of their metabolites were detected, including phase 1
438 metabolites (boscalid 5-hydroxy, thiabendazole 5-hydroxy) and phase 2 metabolites (glucuronide and
439 sulfate conjugates). As expected, all pesticide metabolites were found at higher levels in urine of
440 animals exposed at 10 times the ADI than in urine from animals exposed to the ADI. Overall, more
441 pesticide metabolites or higher levels were detected in exposed CD-fed mice than in exposed WD-fed
442 mice (figure 5A-D).

443 To evaluate the pesticide-detoxifying capacities of CD- and WD-fed mice, we then focused the hepatic
444 RNA sequencing analysis on genes involved in xenobiotic metabolism. The expression profiles of
445 hepatic genes encoding xenobiotic metabolism enzymes in the six experimental animal groups are
446 presented in Figure 5E, F. They reveal that exposure to the pesticide mixture significantly increased
447 the expression of 7 genes in mice fed a CD compared with only 2 in mice fed a WD.
448 Taken together, these results suggest differences in the pharmacokinetics of pesticides, especially in
449 metabolism, between exposed CD- and WD-fed mice. To determine whether extrahepatic pesticide
450 metabolism occurs in WD-fed mice—for example in adipose tissue, which can store lipophilic
451 pollutants—we analyzed WAT for the expression of genes encoding enzymes that regulate
452 detoxification, and of other genes involved in lipolysis, adipogenesis, glucose metabolism, and
453 inflammation (supplementary Figure 5). None of these genes' expression was significantly impacted
454 by pesticide exposure in CD- or WD-fed mice. Similarly, brown adipose tissue (BAT) gene expression of
455 BAT markers and batokines did not significantly differ between pesticide-exposed and unexposed
456 mice, both under WD and CD (supplementary Figure 6). We also evaluated the impact of pesticide
457 mixture exposure on the digestive tract as the first target of dietary pollutants. Expression analysis of
458 genes involved in the structural integrity and permeability of the ileum of the intestine revealed that
459 males fed a CD and exposed to 10 times the ADI of pesticides in a mixture had reduced expression of
460 several genes involved in the ER stress response (*Xbp1s*), antimicrobial activity (*Reg3b* and *Reg3g*), and
461 permeability (*Cldn2*) (supplementary Figure 7). However, the expression of none of these genes was
462 significantly affected by pesticide exposure in WD-fed mice. Together, these results indicate diet-
463 dependent differences in pesticide metabolism, suggesting that the bioavailability of pesticides and/or
464 the animals' detoxifying capacity differ according to the nutritional context.

465 We next evaluated the consequences of chronic exposure to the pesticide mixture on glucose
466 homeostasis. At week 18 of exposure, glucose tolerance, fasting glycemia and insulinemia, and HOMA-
467 IR were not affected by pesticide mixture exposure in mice fed a CD (Figure 6A-D). In contrast, WD-fed
468 mice exposed to the pesticide cocktail at 10ADI exhibited significantly higher glucose intolerance,
469 fasting glycemia, insulinemia, and HOMA-IR compared with animals fed the WD but unexposed (Figure
470 6E-H). To further investigate pesticide mixture–induced glucose homeostasis perturbations in WD-fed
471 mice, we analyzed pancreatic endocrine mass and islet number. Although both parameters were
472 significantly higher in the WD-fed mice than in the CD-fed mice, they did not differ significantly
473 between exposed and unexposed animals under WD (Figure 6I, J). Overall, these results show that
474 dietary exposure to the mixture of pesticides amplified WD-induced glucose homeostasis
475 perturbations that were not associated with a compensatory increase in pancreatic endocrine mass.

476 **Discussion**

477 In this work, we aimed to evaluate the metabolic consequences of a realistic dietary exposure
478 to a mixture of pesticides at their regulatory reference doses, and to determine whether these effects
479 vary depending on the diet composition. The innovative aspects of our study lies in (i) the integration
480 of human epidemiological exposure profiles to guide our pesticide selection (Baudry et al. 2021;
481 Rebouillat et al. 2021), (ii) the use of several *in vitro* assays to identify a pesticide mixture that impact
482 metabolic processes in liver cells, (iii) an *in vivo* study assessing the pertinence of the toxicological
483 reference values (the ADI and 10ADI; corresponding to 1/10 NOAEL) of the 4 selected pesticides in
484 mixture and the influence of diet composition on pesticide mixture-induced effects.

485 The aim of our *in vitro* strategy was to characterize the metabolic effects of the pesticide
486 mixture in liver cells. Our main findings were that the selected pesticide mixture induced gene
487 expression changes, triglyceride accumulation and mitochondrial activity perturbations in IHH cells
488 suggesting its pro-steatotic potency.

489 Our *in vivo* study revealed that the metabolic effects of the pesticide mixture in mice were not
490 uniform, but rather dependent on the type of diet (CD vs WD), highlighting the role of nutritional
491 context in shaping toxicological outcomes. While dietary exposure to the pesticide mixture did not
492 elicit significant alterations in the body weight of mice fed either a CD or a WD, it led to a slight but
493 significant increase in the steatosis score in CD-fed mice. The nonsignificant changes in hepatic
494 triglyceride levels in CD fed mice exposed to the pesticide mixture is not entirely consistent with our
495 *in vitro* studies, which showed a significant increase in triglyceride content in IHH cells upon exposure
496 to the pesticide mixture. However, the changes observed in the hepatic gene expression profile of mice
497 fed a CD support a pro steatotic property of the pesticide mixture. Pathway enrichment analysis of the
498 hepatic transcriptome of CD-fed mice identified fatty acid metabolic processes as the top biological
499 function associated with up-regulated genes in response to pesticide mixture exposure. It cannot be
500 excluded that the 20-week duration of pesticide exposure in our *in vivo* experiment was insufficient to
501 induce detectable phenotypic alterations. In our previous study, we demonstrated that pesticides
502 induced steatosis after 6 months of exposure (Lukowicz et al. 2018). This observation is consistent with
503 other findings that reported pesticide-induced liver damage in mice fed a control diet over extended
504 periods (Dinca et al. 2023; Docea et al. 2018, 2019; Fountoucidou et al. 2019). The discrepancy
505 between *in vivo* and *in vitro* results may stem from interspecies differences or/and from the inability
506 of *in vitro* models to fully capture the complex whole-organism liver responses shaped by interorgan
507 interactions, including those with adipose tissue and the gut microbiota (Djekkoun et al. 2021; Nichols
508 et al. 2024; Velmurugan et al. 2017; Wang et al. 2021).

509 While dietary exposure to the pesticide mixture of WD-fed mice did not induce liver
510 phenotypic and genomic alterations, it exacerbated WD-induced diabetic symptoms, including fasting

511 hyperglycemia, glucose intolerance, and insulin resistance at tenfold ADI dose. These data suggest that
512 exposure to this pesticide mixture may contribute to the development of glucose metabolism
513 disruption in the presence of other risk factors, such as chronic consumption of high-fat foods. Our
514 findings agree with recent studies showing that high-fat dietary intake may enhance the metabolic
515 effects of pesticide exposure. Oral administration of cypermethrin to adult male mice disrupts glucose
516 homeostasis and induces prediabetic symptoms in high-fat diet-fed animals (Wei et al. 2023a). Other
517 studies in rodents have demonstrated that the metabolic perturbations induced by a high-fat diet are
518 potentiated by exposure to low doses of permethrin, chlorpyrifos, perfluorooctanoic acid, and
519 bisphenol A (Attema et al. 2022; Li et al. 2023; Ma et al. 2021; Wang et al. 2021; Xiao et al. 2018). The
520 interaction between dietary factors and pesticide exposure has primarily been demonstrated for
521 individual compounds, with effects varying based on the specific contaminant and exposure duration.
522 However, studies investigating the interplay between diet and pesticide mixtures remain scarce. In a
523 zebrafish model, exposure to a mixture of organochlorine pesticides exacerbated the diabetogenic
524 consequences of a high-fat diet (Lee et al. 2023). Our study extends these findings in mammals,
525 showing that a pesticide mixture can exacerbate WD-induced disruption of glucose homeostasis.

526 Unlike their expression levels in CD-fed mice, the expression levels of xenobiotic metabolizing
527 enzymes were not increased in livers of WD-fed mice following exposure to the pesticide mixture,
528 suggesting reduced pesticide metabolism or the occurrence of extrahepatic pesticide metabolism in
529 WD-fed mice. As urinary profiles of pesticide metabolites were similar between non-exposed and
530 pesticide-exposed WD-fed mice, we hypothesize that pesticides are overall less metabolized in WD-
531 fed mice and may accumulate in other tissues. Previous studies reported that several pesticides,
532 because of their lipophilicity, target adipose tissue (Barrios-Rodríguez et al. 2021; Chang et al. 2016;
533 Jackson et al. 2017; Sousa et al. 2023). Complementary experiments would be necessary to fully
534 elucidate the fate of pesticides in WD-fed mice.

535 The observed hyperglycemia and insulin resistance in WD-fed mice exposed to the pesticide
536 mixture may not be attributed to alterations in gluconeogenesis or glycogen synthesis or decreased
537 glucose uptake in insulin-sensitive tissues, as observed in other studies (Wei et al. 2023b). Indeed,
538 while we did not directly measure hepatic glucose uptake, we found that exposure to the pesticide
539 mixture did not affect the expression of genes involved in glucose synthesis and transport or in insulin
540 signaling in the liver (results not shown). This suggests that the liver may not be the primary target
541 tissue through which the pesticide mixture influences glucose metabolism in WD-fed mice. Whether
542 glucose uptake by skeletal muscle and/or adipose tissue is impaired upon pesticide mixture exposure
543 remains to be determined.

544 T2D occurs when β cells fail to adequately increase insulin secretion to meet demands to
545 counteract insulin resistance, and this failure may be exacerbated by a reduction in β-cell mass over

546 time (Costes et al. 2021). Several pieces of evidence indicated that pancreatic β cells may be targeted
547 by pollutants (Hectors et al. 2011; Hoyeck et al. 2022; Lee et al. 2017). In this study, fasting
548 hyperglycemia and increased fasting insulin in response to WD were both higher in mice exposed to
549 pesticide (10ADI or 1/10 NOAEL) than in non-exposed mice, suggesting that the increased secretory
550 function of pancreatic islet β cells was not sufficient to compensate for insulin resistance. In addition,
551 WD-fed mice exposed to the pesticide mixture showed no differences in islet number and endocrine
552 mass when compared with unexposed mice. While we cannot exclude a difference between the
553 numbers of alpha and beta cells, these data suggest that in WD-fed mice exposed to the pesticide
554 mixture, the endocrine pancreas fails to counteract pesticide-induced glucose intolerance and insulin
555 resistance, in contrast to what occurred in males fed a WD but not exposed.
556 In conclusion, our study demonstrates that chronic dietary exposure to reference doses of
557 each pesticide of this realistic cocktail is associated with significant changes in hepatic gene expression
558 in CD-fed mice and exacerbates WD-induced disruption of glucose homeostasis. This is one of the few
559 studies to demonstrate that dietary context significantly alters the hepatic transcriptomic and
560 metabolic responses to a pesticide mixture in a diet specific manner. The differential response
561 observed between CD- and WD-fed mice emphasizes the complex interplay between environmental
562 contaminants and dietary factors and the importance of considering dietary context when evaluating
563 the metabolic effects of pesticide mixtures. Despite the limitations in translating findings from mice to
564 humans, our results suggest that sensitivity to pesticide exposure may differ according to metabolic
565 status. Given that toxicological reference values ensuring consumer safety are defined for individual
566 pesticides, our findings suggest that their relevance may differ when pesticides are combined in
567 mixtures.
568
569
570
571
572
573
574
575
576
577
578
579
580

581 **Limitations of the study**

582 Although our study assessed the effects of a pesticide mixture administered through food intake, at
583 two toxicological reference doses, on 12 animals per group and in two nutritional contexts, it has some
584 limitations. First, we did not identify the mechanisms underlying the effects of the pesticide mixture
585 on glucose homeostasis or the specific tissue in which pesticides accumulate in WD-fed mice. However,
586 our study provides a comprehensive overview of the observed transcriptomic and phenotypic
587 outcomes, which can serve as a basis for future mechanistic studies. Further mouse studies comparing
588 the effects of the pesticide mixture with those of individual pesticides would be necessary to provide
589 a better understanding of the interactions among the compounds in the mixture. Finally, we did not
590 evaluate the effects of pesticide exposure in female mice. As energy and xenobiotic metabolism in the
591 liver are highly sexually dimorphic, it is likely that the pesticide cocktail could have sex-specific health
592 effects.

593

594 **Acknowledgments**

595 This work was supported by the French Foundation for the Medical Research FRM
596 (ENV202109013962), the Caisse Centrale de la Mutualité Sociale Agricole (AAP Mutualité Sociale
597 Agricole MSA 2022-BIOMEC), the department AlimH of INRAE. We thank Professor Bart Staels and Dr
598 N. Hennuyer (Institut Pasteur, Lille, France) for their generous gift of IHH cells. We thank the EZOP
599 staff, the GeT-Trix Genotoul facility, Metatoul-Metabohub, Anexplo, and We-Met facilities for their
600 help. We also thank the INRAE SAAJ–RAF team (Jouy-en-Josas, France) for its technical support with
601 the pellet preparation. C.R. was supported by FRM (ENV202109013962).

602 **References**

603 Ahmad MF, Ahmad FA, Alsayegh AA, Zeyaullah Md, AlShahrani AM, Muzammil K, et al. 2024.
604 Pesticides impacts on human health and the environment with their mechanisms of action and
605 possible countermeasures. Heliyon 10:e29128; doi:10.1016/j.heliyon.2024.e29128.

606 Akpolat N, Yahsi S, Godekmerdan A, Yalniz M, Demirbag K. 2005. The value of alpha-SMA in the
607 evaluation of hepatic fibrosis severity in hepatitis B infection and cirrhosis development: a
608 histopathological and immunohistochemical study. Histopathology 47:276–280; doi:10.1111/j.1365-
609 2559.2005.02226.x.

610 Arab A, Mostafalou S. 2023. Pesticides and insulin resistance-related metabolic diseases: Evidences
611 and mechanisms. Pesticide Biochemistry and Physiology 195:105521;
612 doi:10.1016/j.pestbp.2023.105521.

613 Arciello M, Gori M, Maggio R, Barbaro B, Tarocchi M, Galli A, et al. 2013. Environmental Pollution: A
614 Tangible Risk for NAFLD Pathogenesis. IJMS 14:22052–22066; doi:10.3390/ijms141122052.

615 Attema B, Janssen AWF, Rijkers D, van Schothorst EM, Hooiveld GJEJ, Kersten S. 2022. Exposure to
616 low-dose perfluorooctanoic acid promotes hepatic steatosis and disrupts the hepatic transcriptome
617 in mice. Molecular Metabolism 66:101602; doi:10.1016/j.molmet.2022.101602.

618 Barrios-Rodríguez R, Pérez-Carrascosa FM, Gómez-Peña C, Mustieles V, Salcedo-Bellido I, Requena P,
619 et al. 2021. Associations of accumulated selected persistent organic pollutants in adipose tissue with
620 insulin sensitivity and risk of incident type-2 diabetes. Environment International 155:106607;
621 doi:10.1016/j.envint.2021.106607.

622 Baudry J, Lelong H, Adriouch S, Julia C, Allès B, Hercberg S, et al. 2018. Association between organic
623 food consumption and metabolic syndrome: cross-sectional results from the NutriNet-Santé study.
624 Eur J Nutr 57:2477–2488; doi:10.1007/s00394-017-1520-1.

625 Baudry J, Rebouillat P, Allès B, Cravedi J-P, Touvier M, Hercberg S, et al. 2021. Estimated dietary
626 exposure to pesticide residues based on organic and conventional data in omnivores, pesco-
627 vegetarians, vegetarians and vegans. Food and Chemical Toxicology 153:112179;
628 doi:10.1016/j.fct.2021.112179.

629 Capitão A, Lyssimachou A, Castro LFC, Santos MM. 2017. Obesogens in the aquatic environment: an
630 evolutionary and toxicological perspective. Environment International 106:153–169;
631 doi:10.1016/j.envint.2017.06.003.

632 Castorina R, Bradman A, McKone TE, Barr DB, Harnly ME, Eskenazi B. 2003. Cumulative
633 organophosphate pesticide exposure and risk assessment among pregnant women living in an
634 agricultural community: a case study from the CHAMACOS cohort. Environ Health Perspect
635 111:1640–1648; doi:10.1289/ehp.5887.

636 Cedergreen N. 2014. Quantifying Synergy: A Systematic Review of Mixture Toxicity Studies within
637 Environmental Toxicology. A. Nazir, ed PLoS ONE 9:e96580; doi:10.1371/journal.pone.0096580.

638 Chang J, Li J, Wang H, Wang Y, Guo B, Yin J, et al. 2016. Tissue distribution, metabolism and hepatic
639 tissue injury in Chinese lizards (Eremias argus) after a single oral administration of lambda-
640 cyhalothrin. Environmental Pollution 218:965–972; doi:10.1016/j.envpol.2016.08.045.

641 Chousidis I, Ellero-Simatos S, Payrastre L, Payros G, Lippi Y, Blaquière M, et al. 2025. Bisphenol
642 analogue exposure at low concentrations modifies heart-brain functions and transcriptomics in
643 zebrafish larvae. Journal of Hazardous Materials 498:140004; doi:10.1016/j.jhazmat.2025.140004.

644 Christen V, Crettaz P, Fent K. 2014. Additive and synergistic antiandrogenic activities of mixtures of
645 azol fungicides and vinclozolin. Toxicology and Applied Pharmacology 279:455–466;
646 doi:10.1016/j.taap.2014.06.025.

647 Costes S, Bertrand G, Ravier MA. 2021. Mechanisms of Beta-Cell Apoptosis in Type 2 Diabetes-Prone
648 Situations and Potential Protection by GLP-1-Based Therapies. IJMS 22:5303;
649 doi:10.3390/ijms22105303.

650 de Sousa G, Nawaz A, Cravedi J-P, Rahmani R. 2014. A Concentration Addition Model to Assess
651 Activation of the Pregnane X Receptor (PXR) by Pesticide Mixtures Found in the French Diet.
652 Toxicological Sciences 141:234–243; doi:10.1093/toxsci/kfu120.

653 Di Tommaso P, Chatzou M, Floden EW, Barja PP, Palumbo E, Notredame C. 2017. Nextflow enables
654 reproducible computational workflows. Nat Biotechnol 35:316–319; doi:10.1038/nbt.3820.

655 Dinca V, Docea AO, Drocas AI, Nikolouzakis TK, Stivaktakis PD, Nikitovic D, et al. 2023. A mixture of 13
656 pesticides, contaminants, and food additives below individual NOAELs produces histopathological
657 and organ weight changes in rats. Arch Toxicol 97:1285–1298; doi:10.1007/s00204-023-03455-x.

658 Djekkoun N, Lalau J-D, Bach V, Depeint F, Khorsi-Cauet H. 2021. Chronic oral exposure to pesticides
659 and their consequences on metabolic regulation: role of the microbiota. Eur J Nutr 60:4131–4149;
660 doi:10.1007/s00394-021-02548-6.

661 Docea AO, Gofita E, Goumenou M, Calina D, Rogoveanu O, Varut M, et al. 2018. Six months exposure
662 to a real life mixture of 13 chemicals' below individual NOAELs induced non monotonic sex-
663 dependent biochemical and redox status changes in rats. Food and Chemical Toxicology 115:470–
664 481; doi:10.1016/j.fct.2018.03.052.

665 Docea AO, Goumenou M, Calina D, Arsene AL, Dragoi CM, Gofita E, et al. 2019. Adverse and hormetic
666 effects in rats exposed for 12 months to low dose mixture of 13 chemicals: RLRS part III. Toxicology
667 Letters 310:70–91; doi:10.1016/j.toxlet.2019.04.005.

668 European Food Safety Authority (EFSA), Carrasco Cabrera L, Di Piazza G, Dujardin B, Marchese E,
669 Medina Pastor P. 2024. The 2022 European Union report on pesticide residues in food. EFS2 22;
670 doi:10.2903/j.efsa.2024.8753.

671 Expertise Collective Inserm. 2013. *Pesticides: Effets sur la santé.* Les éditions Inserm. Paris.

672 Expertise Collective Inserm. 2021. Pesticides et effets sur la santé. Nouvelles données. *Editions EDP*
673 *science*.

674 Fountoucidou P, Veskoukis AS, Kerasioti E, Docea AO, Taitzoglou IA, Liesivuori J, et al. 2019. A mixture
675 of routinely encountered xenobiotics induces both redox adaptations and perturbations in blood and
676 tissues of rats after a long-term low-dose exposure regimen: The time and dose issue. Toxicology
677 Letters 317:24–44; doi:10.1016/j.toxlet.2019.09.015.

678 Friedman SL, Neuschwander-Tetri BA, Rinella M, Sanyal AJ. 2018. Mechanisms of NAFLD
679 development and therapeutic strategies. Nat Med 24:908–922; doi:10.1038/s41591-018-0104-9.

Fujino C, Watanabe Y, Sanoh S, Nakajima H, Uramaru N, Kojima H, et al. 2019. Activation of PXR, CAR and PPARα by pyrethroid pesticides and the effect of metabolism by rat liver microsomes. Heliyon 5:e02466; doi:10.1016/j.heliyon.2019.e02466.

Groswald AM, Gripshover TC, Watson WH, Wahlang B, Luo J, Jophlin LL, et al. 2023. Investigating the Acute Metabolic Effects of the N-Methyl Carbamate Insecticide, Methomyl, on Mouse Liver. Metabolites 13:901; doi:10.3390/metabo13080901.

He B, Ni Y, Jin Y, Fu Z. 2020. Pesticides-induced energy metabolic disorders. Science of The Total Environment 729:139033; doi:10.1016/j.scitotenv.2020.139033.

Hectors TLM, Vanparys C, van der Ven K, Martens GA, Jorens PG, Van Gaal LF, et al. 2011. Environmental pollutants and type 2 diabetes: a review of mechanisms that can disrupt beta cell function. Diabetologia 54:1273–1290; doi:10.1007/s00125-011-2109-5.

Hernández AF, Parrón T, Tsatsakis AM, Requena M, Alarcón R, López-Guarnido O. 2013. Toxic effects of pesticide mixtures at a molecular level: Their relevance to human health. Toxicology 307:136–145; doi:10.1016/j.tox.2012.06.009.

Hoyeck MP, Matteo G, MacFarlane EM, Perera I, Bruin JE. 2022. Persistent organic pollutants and β-cell toxicity: a comprehensive review. American Journal of Physiology-Endocrinology and Metabolism 322:E383–E413; doi:10.1152/ajpendo.00358.2021.

Jabłońska-Trypuć. 2017. The impact of pesticides on oxidative stress level in human organism and their activity as an endocrine disruptor. Journal of Environmental Science and Health, Part B.

Jackson E, Shoemaker R, Larian N, Cassis L. 2017. Adipose Tissue as a Site of Toxin Accumulation. In: *Comprehensive Physiology* (R. Terjung, ed). Wiley. 1085–1135.

Kesse-Guyot E, Baudry J, Assmann KE, Galan P, Hercberg S, Lairon D. 2017. Prospective association between consumption frequency of organic food and body weight change, risk of overweight or obesity: results from the NutriNet-Santé Study. Br J Nutr 117:325–334; doi:10.1017/s0007114517000058.

Kesse-Guyot E, Rebouillat P, Payrastre L, Allès B, Fezeu LK, Druesne-Pecollo N, et al. 2020. Prospective association between organic food consumption and the risk of type 2 diabetes: findings from the NutriNet-Santé cohort study. Int J Behav Nutr Phys Act 17; doi:10.1186/s12966-020-01038-y.

Knebel C, Kebben J, Eberini I, Palazzolo L, Hammer HS, Süssmuth RD, et al. 2018a. Propiconazole is an activator of AHR and causes concentration additive effects with an established AHR ligand. Arch Toxicol 92:3471–3486; doi:10.1007/s00204-018-2321-x.

Knebel C, Kebben J, Eberini I, Palazzolo L, Hammer HS, Süssmuth RD, et al. 2018b. Propiconazole is an activator of AHR and causes concentration additive effects with an established AHR ligand. Arch Toxicol 92:3471–3486; doi:10.1007/s00204-018-2321-x.

Lee H, Gao Y, Kim JK, Shin S, Choi M, Hwang Y, et al. 2023. Synergetic effects of concurrent chronic exposure to a mixture of OCPs and high-fat diets on type 2 diabetes and beneficial effects of caloric restriction in female zebrafish. Journal of Hazardous Materials 446:130659; doi:10.1016/j.jhazmat.2022.130659.

Lee Y-M, Ha C-M, Kim S-A, Thoudam T, Yoon Y-R, Kim D-J, et al. 2017. Low-Dose Persistent Organic Pollutants Impair Insulin Secretory Function of Pancreatic b-Cells: Human and In Vitro Evidence. 66.

721 Léger T, Balaguer P, Le Hégarat L, Fessard V. 2023. Fate and PPARγ and STATs-driven effects of the
722 mitochondrial complex I inhibitor tebufenpyrad in liver cells revealed with multi-omics. Journal of
723 Hazardous Materials 442:130083; doi:10.1016/j.jhazmat.2022.130083.

724 Leroux P. 2003. Modes d'action des produits phytosanitaires sur les organismes pathogènes des
725 plantes. Comptes Rendus Biologies 326:9–21; doi:10.1016/S1631-0691(03)00005-2.

726 Li J, Li X, Zhang Z, Cheng W, Liu G, Zhao G. 2023. High-Fat Diet Aggravates the Disorder of Glucose
727 Metabolism Caused by Chlorpyrifos Exposure in Experimental Rats. Foods 12:816;
728 doi:10.3390/foods12040816.

729 Li W, Xiao H, Wu H, Pan C, Deng K, Xu X, et al. 2022. Analysis of environmental chemical mixtures and
730 nonalcoholic fatty liver disease: NHANES 1999–2014. Environmental Pollution 311:119915;
731 doi:10.1016/j.envpol.2022.119915.

732 Lichtenstein D, Luckert C, Alarcan J, de Sousa G, Gioutlakis M, Katsanou ES, et al. 2020. An adverse
733 outcome pathway-based approach to assess steatotic mixture effects of hepatotoxic pesticides in
734 vitro. Food and Chemical Toxicology 139:111283; doi:10.1016/j.fct.2020.111283.

735 Lippi Y, Soubès F. 2023. MATRiX: a shiny application for Mining and functional Analysis of
736 TRanscriptomics data.; doi:10.17180/DJ0G-5F33.

737 Lukowicz C, Ellero-Simatos S, Régnier M, Polizzi A, Lasserre F, Montagner A, et al. 2018. Metabolic
738 Effects of a Chronic Dietary Exposure to a Low-Dose Pesticide Cocktail in Mice: Sexual Dimorphism
739 and Role of the Constitutive Androstane Receptor. Environ Health Perspect 126:067007;
740 doi:10.1289/EHP2877.

741 Ma Q, Deng P, Lin M, Yang L, Li L, Guo L, et al. 2021. Long-term bisphenol A exposure exacerbates
742 diet-induced prediabetes via TLR4-dependent hypothalamic inflammation. Journal of Hazardous
743 Materials 402:123926; doi:10.1016/j.jhazmat.2020.123926.

744 Mardinoglu A. 2018. Systems biology in hepatology: approaches and applications.

745 Mellor CL, Steinmetz FP, Cronin MTD. 2016. The identification of nuclear receptors associated with
746 hepatic steatosis to develop and extend adverse outcome pathways. Critical Reviews in Toxicology
747 46:138–152; doi:10.3109/10408444.2015.1089471.

748 Mesnage R, Mahmud N, Mein CA, Antoniou MN. 2021. Alterations in small RNA profiles in liver
749 following a subchronic exposure to a low-dose pesticide mixture in Sprague-Dawley rats. Toxicology
750 Letters 353:20–26; doi:10.1016/j.toxlet.2021.10.001.

751 Nichols RG, Rimal B, Hao F, Peters JM, Davenport ER, Patterson AD. 2024. Chlorpyrifos modulates the
752 mouse gut microbiota and metabolic activity. Environment International 192:109022;
753 doi:10.1016/j.envint.2024.109022.

754 Podechard N, Ducheix S, Polizzi A, Lasserre F, Montagner A, Legagneux V, et al. 2018. Dual extraction
755 of mRNA and lipids from a single biological sample. Sci Rep 8:7019; doi:10.1038/s41598-018-25332-
756 9.

757 Rajak, S., Raza,z, Tewari, A. 2022. Environmental Toxicants and NAFLD: A Neglected yet Significant
758 Relationship. Dig Dis Sci.

759 Rebouillat P, Vidal R, Cravedi J-P, Taupier-Letage B, Debrauwer L, Gamet-Payrastre L, et al. 2021.
760 Estimated dietary pesticide exposure from plant-based foods using NMF-derived profiles in a large
761 sample of French adults. Eur J Nutr 60:1475–1488; doi:10.1007/s00394-020-02344-8.

762 Rebouillat P, Vidal R, Cravedi J-P, Taupier-Letage B, Debrauwer L, Gamet-Payrastre L, et al. 2022.
763 Prospective association between dietary pesticide exposure profiles and type 2 diabetes risk in the
764 NutriNet-Santé cohort. Environ Health 21:57; doi:10.1186/s12940-022-00862-y.

765 Rives C, Fougerat A, Ellero-Simatos S, Loiseau N, Guillou H, Gamet-Payrastre L, et al. 2020. Oxidative
766 Stress in NAFLD: Role of Nutrients and Food Contaminants. Biomolecules 10:1702;
767 doi:10.3390/biom10121702.

768 Roustan A, Aye M, De Meo M, Di Giorgio C. 2014. Genotoxicity of mixtures of glyphosate and atrazine
769 and their environmental transformation products before and after photoactivation. Chemosphere
770 108:93–100; doi:10.1016/j.chemosphere.2014.02.079.

771 Schmidt FF, Lichtenstein D, Planatscher H, Mentz A, Kalinowski J, Steinhilber AE, et al. 2021. Pesticide
772 mixture effects on liver protein abundance in HepaRG cells. Toxicology 458:152839;
773 doi:10.1016/j.tox.2021.152839.

774 Sousa S, Rede D, Cruz Fernandes V, Pestana D, Faria G, Delerue-Matos C, et al. 2023. Accumulation of
775 organophosphorus pollutants in adipose tissue of obese women - metabolic alterations.
776 Environmental Research 239:117337; doi:10.1016/j.envres.2023.117337.

777 Tait S, Lori G, Tassinari R, La Rocca C, Maranghi F. 2022. In Vitro Assessment and Toxicological
778 Prioritization of Pesticide Mixtures at Concentrations Derived from Real Exposure in Occupational
779 Scenarios. IJERPH 19:5202; doi:10.3390/ijerph19095202.

780 Velmurugan G, Ramprasath T, Swaminathan K, Mithieux G, Rajendhran J, Dhivakar M, et al. 2017. Gut
781 microbial degradation of organophosphate insecticides-induces glucose intolerance via
782 gluconeogenesis. Genome Biol 18:8; doi:10.1186/s13059-016-1134-6.

783 Vinken M, Knapen D, Vergauwen L, Hengstler JG, Angrish M, Whelan M. 2017. Adverse outcome
784 pathways: a concise introduction for toxicologists. Arch Toxicol 91:3697–3707; doi:10.1007/s00204-
785 017-2020-z.

786 Wahlang B, Jin J, Beier JI, Hardesty JE, Daly EF, Schnegelberger RD, et al. 2019. Mechanisms of
787 Environmental Contributions to Fatty Liver Disease. Curr Envir Health Rpt 6:80–94;
788 doi:10.1007/s40572-019-00232-w.

789 Wang B, Tsakiridis EE, Zhang S, Llanos A, Desjardins EM, Yabut JM, et al. 2021. The pesticide
790 chlorpyrifos promotes obesity by inhibiting diet-induced thermogenesis in brown adipose tissue. Nat
791 Commun 12:5163; doi:10.1038/s41467-021-25384-y.

792 Wang R, Yang X, Wang T, Kou R, Liu P, Huang Y, et al. 2023. Synergistic effects on oxidative stress,
793 apoptosis and necrosis resulting from combined toxicity of three commonly used pesticides on
794 HepG2 cells. Ecotoxicology and Environmental Safety 263:115237;
795 doi:10.1016/j.ecoenv.2023.115237.

796 Wang X, Lu Q, Guo J, Ares I, Martínez M, Martínez-Larrañaga M-R, et al. 2022. Oxidative Stress and
797 Metabolism: A Mechanistic Insight for Glyphosate Toxicology. Annu Rev Pharmacol Toxicol 62:617–
798 639; doi:10.1146/annurev-pharmtox-020821-111552.

799 Wei Y, Liu W, Liu J. 2023a. Environmentally relevant exposure to cypermethrin aggravates diet-
800 induced diabetic symptoms in mice: The interaction between environmental chemicals and diet.
801 Environment International 178:108090; doi:10.1016/j.envint.2023.108090.

802 Wei Y, Wang L, Liu J. 2023b. The diabetogenic effects of pesticides: Evidence based on
803 epidemiological and toxicological studies. Environmental Pollution 331:121927;
804 doi:10.1016/j.envpol.2023.121927.

805 Xiao X, Sun Q, Kim Y, Yang S-H, Qi W, Kim D, et al. 2018. Exposure to permethrin promotes high fat
806 diet-induced weight gain and insulin resistance in male C57BL/6J mice. Food and Chemical Toxicology
807 111:405–416; doi:10.1016/j.fct.2017.11.047.

808 Yang D, Sun X, Wei X, Zhang B, Fan X, Du H, et al. 2023. Lambda-cyhalothrin induces lipid
809 accumulation in mouse liver is associated with AMPK inactivation. Food and Chemical Toxicology
810 172:113563; doi:10.1016/j.fct.2022.113563.

811 Yang JS, Park Y. 2018. Insecticide Exposure and Development of Nonalcoholic Fatty Liver Disease. J
812 Agric Food Chem 66:10132–10138; doi:10.1021/acs.jafc.8b03177.

813 Zhou Y, Zhou B, Pache L, Chang M, Khodabakhshi AH, Tanaseichuk O, et al. 2019. Metascape provides
814 a biologist-oriented resource for the analysis of systems-level datasets. Nat Commun 10:1523;
815 doi:10.1038/s41467-019-09234-6.

816

817 **Figure legends**
818
819 **Figure 1: Selection of candidate pesticides.**
820
821 **Figure 2: Impact of the mixture of 4 pesticides on IHH cell metabolism.**
822 **(A)** Impact of the pesticide mixture on nuclear receptor activation in IHH cells. Relative expression of
823 CYP4A11, CYP2B6, CYP3A4, SREBP1c and CYP1A1 mRNAs in IHH cells exposed to the mixture (ITBL) at
824 30 µM for each pesticide for 24 h (n = 6/condition). **(B-E)** Impact of the pesticide mixture on gene
825 expression in IHH cells. Data from a microarray experiment performed with IHH cells treated with the
826 pesticide mixture (ITBL) at 30 µM for each pesticide in the mixture for 24 h (n = 6/condition). (**B**)
827 Principal component analysis (PCA) score plots of the IHH transcriptomic dataset. (**C**) Number of
828 differentially up- and downregulated genes in exposed vs. control untreated cells. (**D**) Heatmap and
829 hierarchical clustering showing the definition of 2 gene clusters ($p \leq 0.05$ and fold change >1.5). (**E**)
830 Pathway and transcription factor enrichment analysis in each cluster. For each sample, the raw data
831 were normalized to the average value of all the samples. **(F)** Impact of the pesticide mixture on
832 triglyceride content in IHH cells**.** Triglyceride content in IHH cells treated with the pesticide mixture at
833 30 µM for 10 days (n = 3-4). **(G, H)** Impact of the pesticide mixture on mitochondrial respiration in IHH
834 cells**.** (**G**) Oxygen consumption rate (OCR) profiles of IHH cells treated with the pesticide mixture at 30
835 µM for 24 h (n = 3-4). (**H**) Basal respiration, maximal respiration, proton leak and ATP production of
836 IHH cells treated with the pesticide mixture. Data are presented as the mean ± SEM. * Treatment
837 effect, * $p < 0.05$, ** $p < 0.01$, *** $p < 0.001$. (A, F, H) Unpaired parametric T test; (G)Two-way ANOVA
838 multiple comparisons test.
839
840
841 **Figure 3: Pesticide mixture exposure does not influence mouse body weight, regardless of diet.**
842 **(A)** Experimental design. Eight-week-old male C57BL6J mice were fed a control diet (CD) or a Western
843 diet (WD) for 5 weeks. Both groups were then divided into 3 subgroups: one fed a diet containing the
844 mixture of 4 pesticides (ITBL) and exposed to the acceptable daily intake (CD- or WD-ADI) of each
845 pesticide; one fed a diet containing the mixture of 4 pesticides (ITBL) and exposed to 10 times the ADI
846 (CD- or WD-10-ADI) of each pesticide; and one not exposed to pesticides (CD or WD) for 20 weeks (n =
847 12 animals per group). **(B, C)** Body weight in each group from week 0 prior to exposure through 25
848 weeks. The bar graphs show the body weight gain at the end of the experiment. **(D-G)** Relative
849 subcutaneous (sc) (**D**, **F**) and epididymal (pg) (**E**, **G**) white adipose tissue weight in each group of mice
850 (n = 12 per group). Data are presented as the mean ± SEM (body weight follow-up (B, C), two-way
851 ANOVA followed by a Tuckey's post-hoc test; bar graphs (B-G), one-way ANOVA followed by a Tuckey's
852 post-hoc test).
853
854 **Figure 4: Pesticide mixture exposure changes hepatic gene expression in a diet-dependent manner.**
855 **(A-D)** Relative liver weight and plasma alanine aminotransferase (ALT) levels of CD-fed (**A**, **B**) and WD-
856 fed (**C**, **D**) mice in each group (n = 12 per group). **(E)** Representative histological sections (magnification
857 ×100) of liver stained with hematoxylin and eosin (H&E) and estimated liver steatosis score in each
858 group (n = 12 per group). **(F)** Hepatic triglyceride content in each group (n = 12 per group). **(G-K)** Data
859 from an RNA-seq experiment performed with liver samples from each group of mice (n = 8/group).
860 Principal component analysis (PCA) score plots of liver transcriptomic dataset in CD- (**G**) and WD-fed
861 mice (**H**). Number of differentially up- and downregulated genes in CD- and WD-fed mice unexposed
862 vs. exposed to ADI, unexposed vs. exposed to 10ADI or exposed to ADI vs. exposed to 10ADI (n.s.,
863 nonsignificant) (**I**). Hierarchical clustering showing the definition of 2 gene clusters ($p \leq 0.05$ and fold
864 change >1) (**J**) and pathway and transcription factor enrichment analysis in each cluster (**K**). Data are
865 presented as the mean ± SEM. * Treatment effect, * $p < 0.05$, one-way ANOVA followed by Tukey's
866 post-hoc test (A-D, G); Kruskal- Wallis followed by Dunn's post-hoc test (F).
867

868 **Figure 5: Urinary pesticide metabolites and mRNA expression level of genes involved in xenobiotic**
869 **metabolism.**
870 **(A-D)** Normalized intensities of one metabolite of imazalil (**A**), two metabolites of thiabendazole (**B**),
871 boscalid and two of its metabolites (**C**), one metabolite of lambda-cyhalothrin (**D**) measured by UHPLC-
872 HRMS in 24 h urine samples of each group of mice (n = 8 per group). Data are presented as the mean
873 ± SEM. *Treatment effect, *$p < 0.05$, **$p < 0.01$ (Kruskal- Wallis followed by Dunn's post-hoc test);
874 n.d.: non-detected metabolites. **(E, F)** mRNA expression of hepatic genes involved in xenobiotic
875 metabolism in CD- (**E**) and WD-fed (**F**) mice exposed and non-exposed to the pesticide mixture (n = 8
876 per group). Data are presented as the mean ± SEM. *Exposed vs. non-exposed mice, *$p < 0.05$, **$p <$
877 0.01 (one-way ANOVA followed by Tuckey's post-hoc test).
878
879 **Figure 6: Pesticide mixture exposure exacerbates WD-induced glucose homeostasis perturbations.**
880 **(A, E)** Oral glucose tolerance test (OGTT) performed after 18 weeks of pesticide exposure in CD- (**A**)
881 and WD-fed (**E**) mice in each group (n = 12 per group) and area under the curve (AUC) representing
882 OGTT results. **(B, F)** Fasting glycemia. **(C, G)** Fasting insulinemia. **(D, H)** HOMAR-IR. **(I)** Islet number per
883 mm^2 of pancreas. **(J)** Percent of section area occupied by islets. Data are presented as the mean ± SEM.
884 * Exposed vs. non-exposed mice, * $p < 0.05$, ** $p < 0.01$; # exposed ADI vs. exposed 10ADI, # $p < 0.05$,
885 ## $p < 0.01$ (Two-way ANOVA followed by Tukey's post-hoc test (A, E); One-way Anova followed by a
886 Tuckey's post-hoc test (bar graphs A-J).

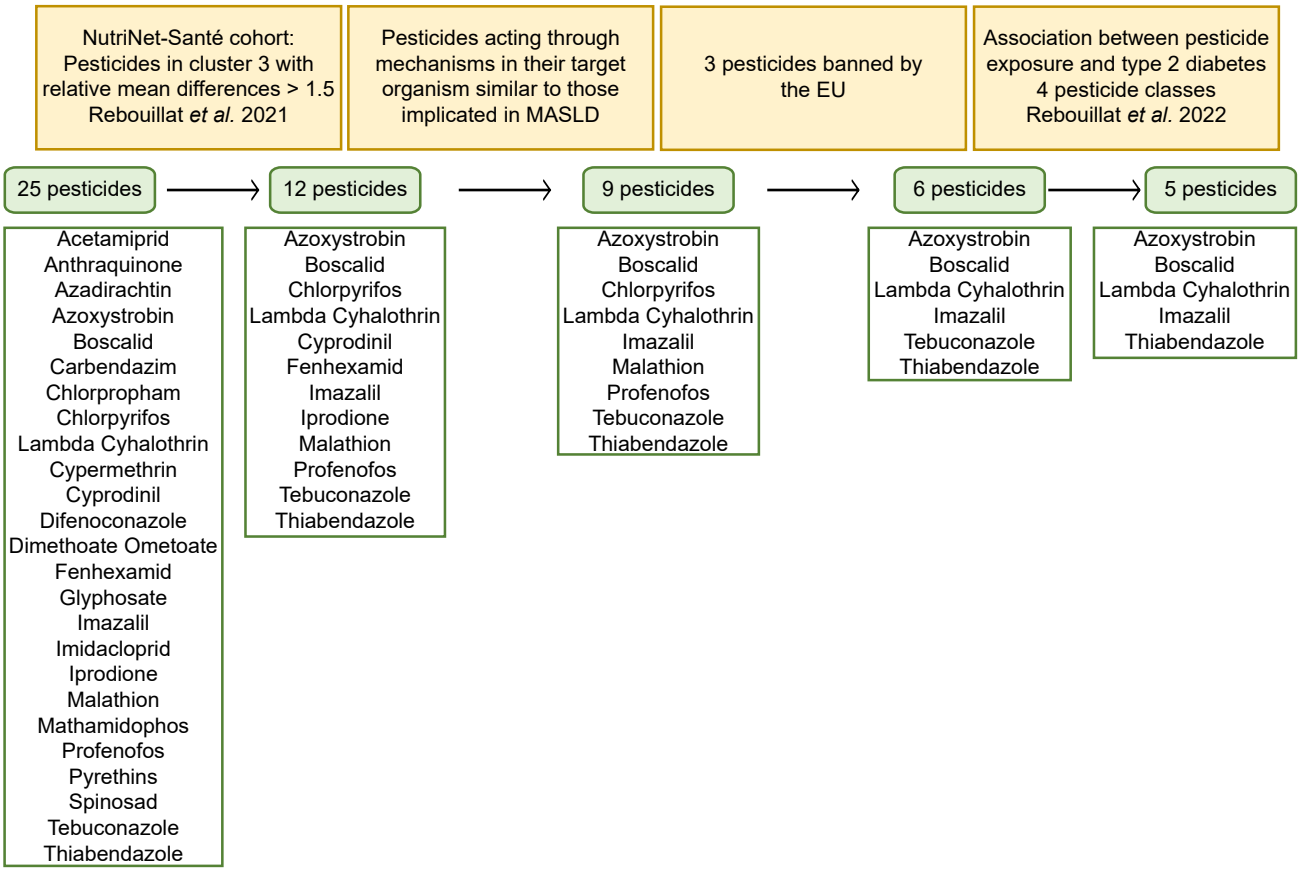
NutriNet-Santé cohort: Pesticides in cluster 3 with relative mean differences > 1.5 Rebouillat *et al.* 2021
Pesticides acting through mechanisms in their target organism similar to those implicated in MASLD
3 pesticides banned by the EU
Association between pesticide exposure and type 2 diabetes 4 pesticide classes Rebouillat *et al.* 2022
25 pesticides
Acetamiprid
Anthraquinone
Azadirachtin
Azoxystrobin
Boscalid
Carbendazim
Chlorpropham
Chlorpyrifos
Lambda Cyhalothrin
Cypermethrin
Cyprodinil
Difenoconazole
Dimethoate Ometoate
Fenhexamid
Glyphosate
Imazalil
Imidacloprid
Iprodione
Malathion
Mathamidophos
Profenofos
Pyrethins
Spinosad
Tebuconazole
Thiabendazole
12 pesticides
Azoxystrobin
Boscalid
Chlorpyrifos
Lambda Cyhalothrin
Cyprodinil
Fenhexamid
Imazalil
Iprodione
Malathion
Profenofos
Tebuconazole
Thiabendazole
9 pesticides
Azoxystrobin
Boscalid
Chlorpyrifos
Lambda Cyhalothrin
Imazalil
Malathion
Profenofos
Tebuconazole
Thiabendazole
6 pesticides
Azoxystrobin
Boscalid
Lambda Cyhalothrin
Imazalil
Tebuconazole
Thiabendazole
5 pesticides
Azoxystrobin
Boscalid
Lambda Cyhalothrin
Imazalil
Thiabendazole

Figure 1

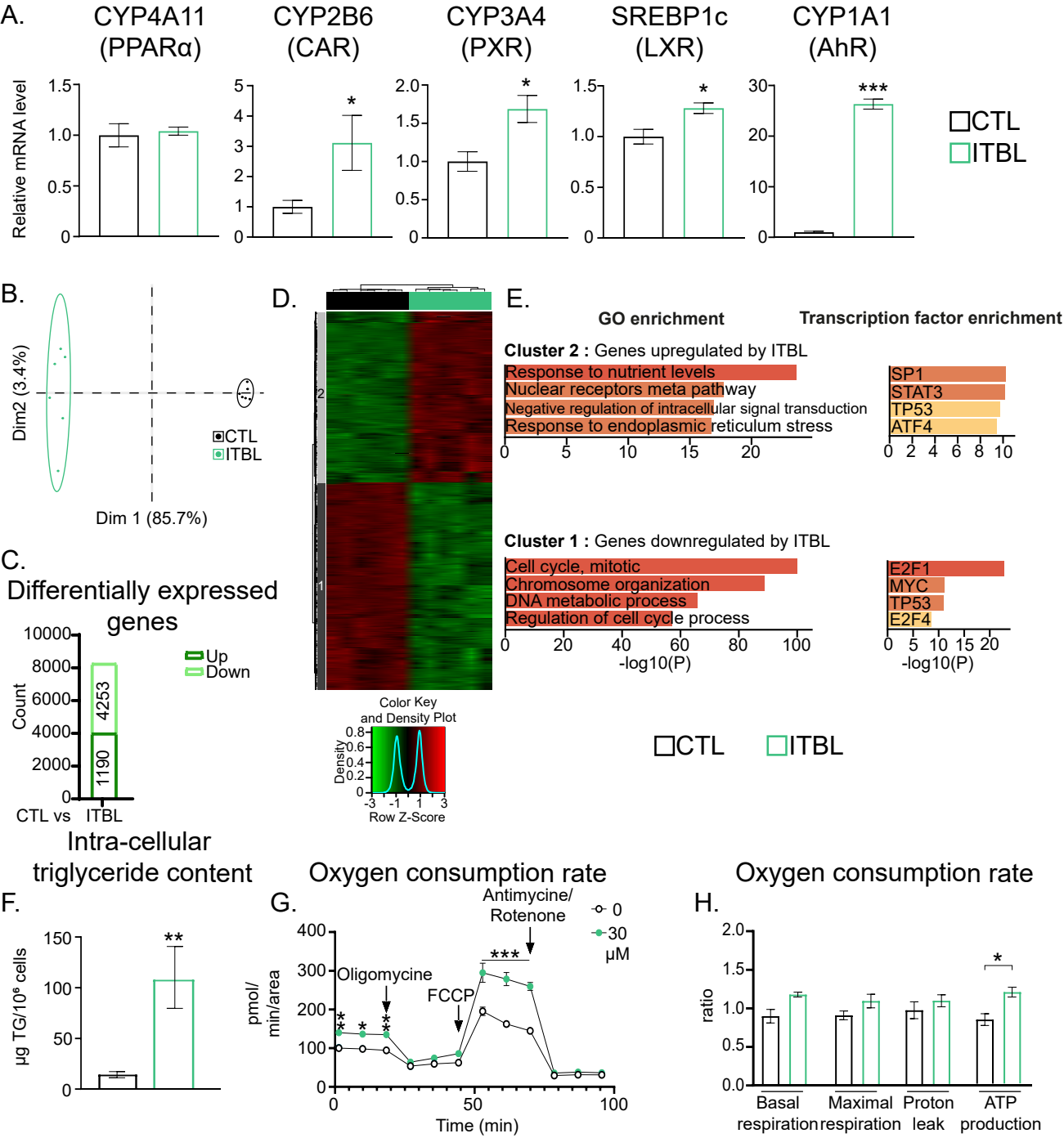
A.
CYP4A11 (PPARα)
CYP2B6 (CAR)
CYP3A4 (PXR)
SREBP1c (LXR)
CYP1A1 (AhR)
Relative mRNA level
CTL
ITBL
B.
Dim2 (3.4%)
Dim 1 (85.7%)
CTL
ITBL
C.
Differentially expressed genes
Up
Down
Count
4253
1190
CTL vs ITBL
D.
Color Key and Density Plot
Density
Row Z-Score
E.
GO enrichment
Transcription factor enrichment
Cluster 2 : Genes upregulated by ITBL
Response to nutrient levels
Nuclear receptors meta pathway
Negative regulation of intracellular signal transduction
Response to endoplasmic reticulum stress
SP1
STAT3
TP53
ATF4
Cluster 1 : Genes downregulated by ITBL
Cell cycle, mitotic
Chromosome organization
DNA metabolic process
Regulation of cell cycle process
E2F1
MYC
TP53
E2F4
-log10(P)
CTL
ITBL
Intra-cellular triglyceride content
F.
µg TG/10⁶ cells
Oxygen consumption rate
G.
Antimycine/ Rotenone
0
30 µM
Oligomycine
FCCP
pmol/ min/area
Time (min)
Oxygen consumption rate
H.
ratio
Basal respiration
Maximal respiration
Proton leak
ATP production

Figure 2

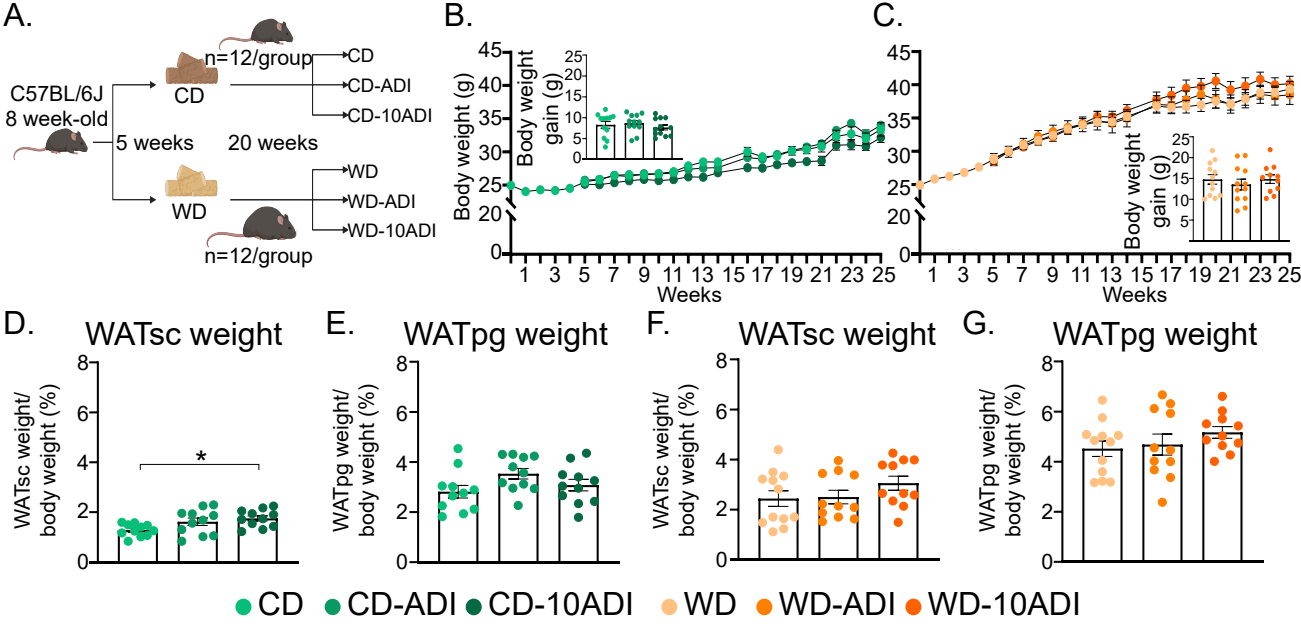
A.
C57BL/6J
8 week-old
5 weeks
20 weeks
CD
WD
n=12/group
CD
CD-ADI
CD-10ADI
WD
WD-ADI
WD-10ADI
n=12/group
B.
Body weight (g)
Body weight gain (g)
Weeks
C.
Body weight gain (g)
Weeks
D.
WATsc weight
WATsc weight/ body weight (%)
E.
WATpg weight
WATpg weight/ body weight (%)
F.
WATsc weight
WATsc weight/ body weight (%)
G.
WATpg weight
WATpg weight/ body weight (%)
CD
CD-ADI
CD-10ADI
WD
WD-ADI
WD-10ADI

Figure 3

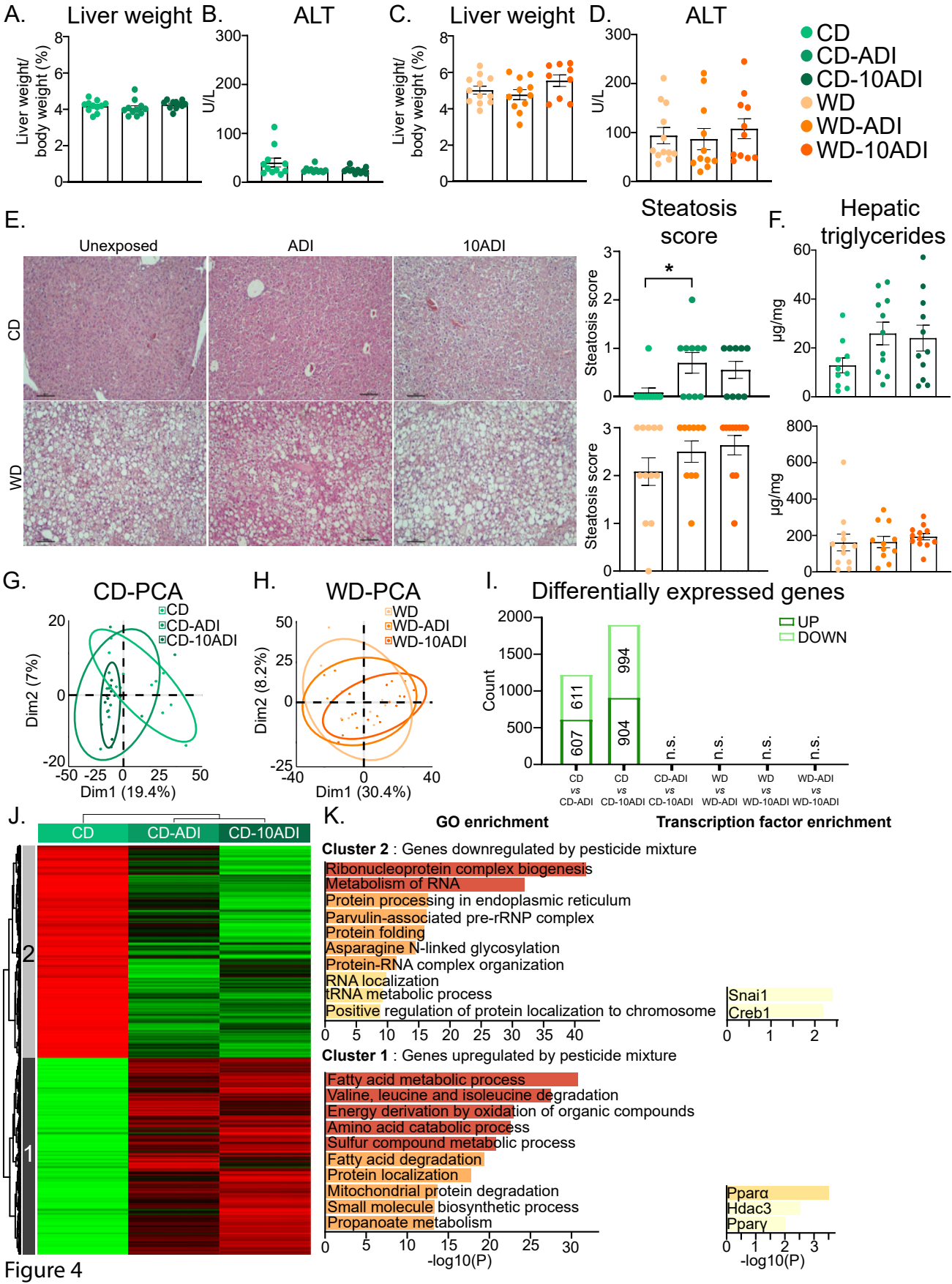
A.
Liver weight
Liver weight/ body weight (%)
B.
ALT
U/L
C.
Liver weight
Liver weight/ body weight (%)
D.
ALT
U/L
CD
CD-ADI
CD-10ADI
WD
WD-ADI
WD-10ADI
E.
Unexposed
ADI
10ADI
CD
WD
Steatosis score
Steatosis score
F.
Hepatic triglycerides
µg/mg
G.
CD-PCA
CD
CD-ADI
CD-10ADI
Dim1 (19.4%)
Dim2 (7%)
H.
WD-PCA
WD
WD-ADI
WD-10ADI
Dim1 (30.4%)
Dim2 (8.2%)
I.
Differentially expressed genes
UP
DOWN
Count
607
611
904
994
n.s.
CD vs CD-ADI
CD vs CD-10ADI
CD-ADI vs CD-10ADI
WD vs WD-ADI
WD vs WD-10ADI
WD-ADI vs WD-10ADI
J.
CD
CD-ADI
CD-10ADI
2
1
K.
GO enrichment
Transcription factor enrichment
Cluster 2 : Genes downregulated by pesticide mixture
Ribonucleoprotein complex biogenesis
Metabolism of RNA
Protein processing in endoplasmic reticulum
Parvulin-associated pre-rRNP complex
Protein folding
Asparagine N-linked glycosylation
Protein-RNA complex organization
RNA localization
tRNA metabolic process
Positive regulation of protein localization to chromosome
Snai1
Creb1
Cluster 1 : Genes upregulated by pesticide mixture
Fatty acid metabolic process
Valine, leucine and isoleucine degradation
Energy derivation by oxidation of organic compounds
Amino acid catabolic process
Sulfur compound metabolic process
Fatty acid degradation
Protein localization
Mitochondrial protein degradation
Small molecule biosynthetic process
Propanoate metabolism
Pparα
Hdac3
Pparγ
-log10(P)
-log10(P)

Figure 4

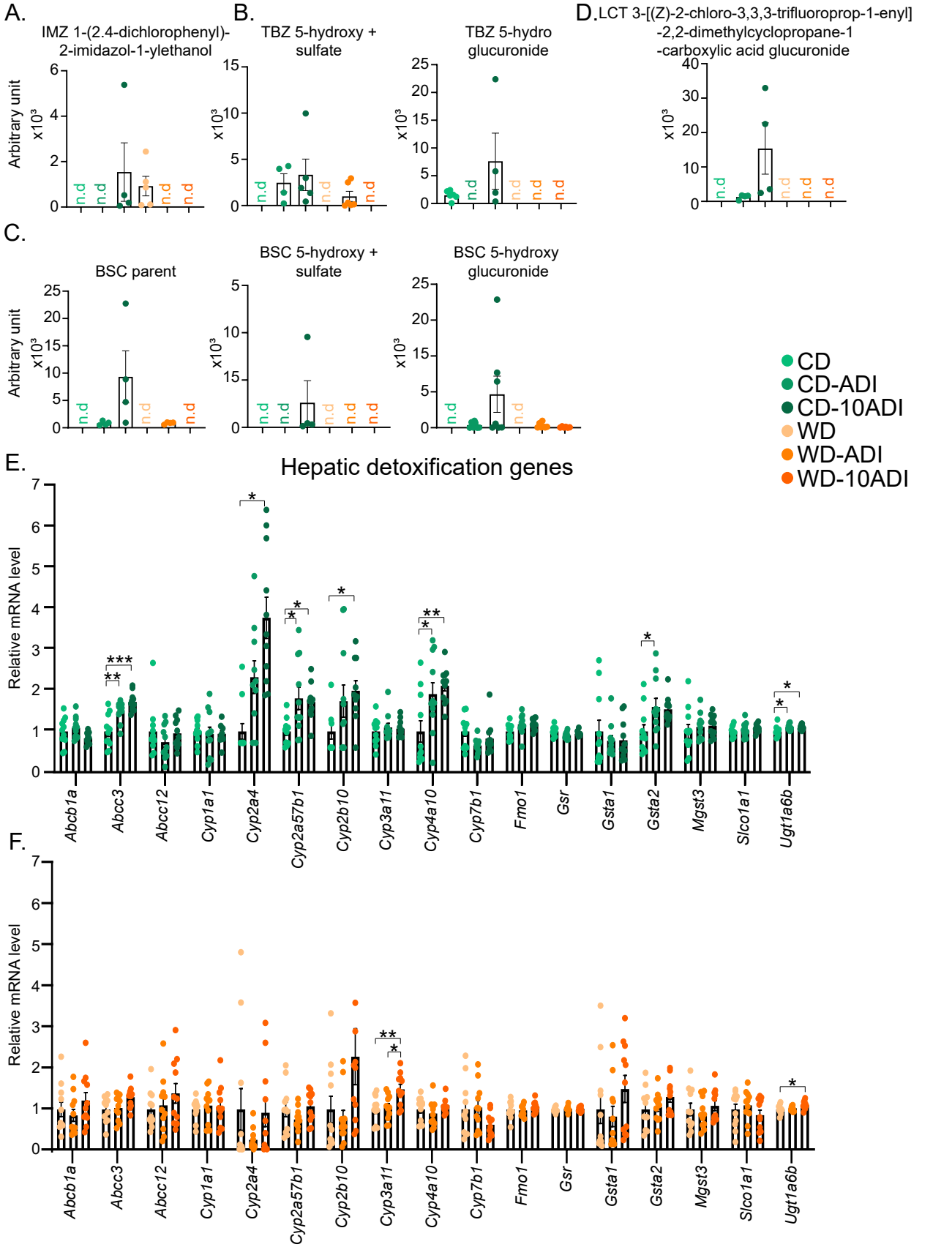
A.
IMZ 1-(2.4-dichlorophenyl)-2-imidazol-1-ylethanol
B.
TBZ 5-hydroxy + sulfate
TBZ 5-hydro glucuronide
D.
LCT 3-[(Z)-2-chloro-3,3,3-trifluoroprop-1-enyl]-2,2-dimethylcyclopropane-1-carboxylic acid glucuronide
Arbitrary unit
x10³
n.d
C.
BSC parent
BSC 5-hydroxy + sulfate
BSC 5-hydroxy glucuronide
CD
CD-ADI
CD-10ADI
WD
WD-ADI
WD-10ADI
E.
Hepatic detoxification genes
Relative mRNA level
Abcb1a
Abcc3
Abcc12
Cyp1a1
Cyp2a4
Cyp2a57b1
Cyp2b10
Cyp3a11
Cyp4a10
Cyp7b1
Fmo1
Gsr
Gsta1
Gsta2
Mgst3
Slco1a1
Ugt1a6b
F.

Figure 5

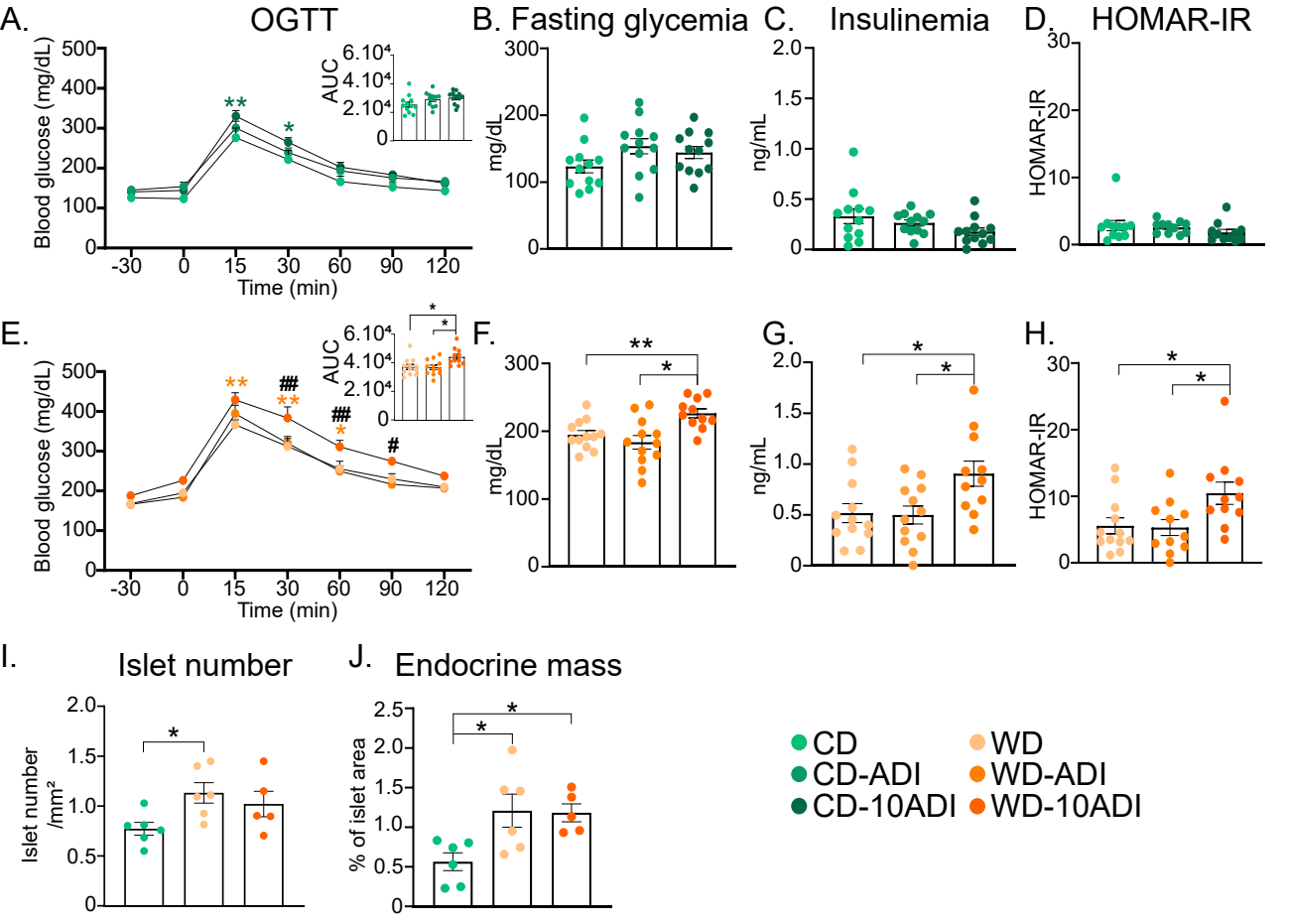
A.
OGTT
Blood glucose (mg/dL)
Time (min)
AUC
B. Fasting glycemia
mg/dL
C.
Insulinemia
ng/mL
D.
HOMAR-IR
E.
F.
G.
H.
I.
Islet number
Islet number /mm²
J.
Endocrine mass
% of islet area
CD
CD-ADI
CD-10ADI
WD
WD-ADI
WD-10ADI

Figure 6